Flexible energy systems Leveraging the Optimal integration of EVs deployment Wave

Grant Agreement Nº: 101056730

Deliverable 4.3

Advanced flexibility management system description and functionalities

Authors: Giuseppe Silano (RSE), Tomas Montes (IREC), Ferran Pinsach (IREC), Lucía Igualada (IREC), Josh Eichman (IREC), István Bara (TUD), and Gautham Ram Chandra Mouli (TUD)

[Ricerca sul Sistema Energetico (RSE), Fundacio Institut De Recerca De L'energia De Catalunya (IREC), and Technical University of Delft (TUD)]

Website FLOW

Funded by the European Union

Project funded by

Schweizerische Eidgenossenschaft
Confédération suisse
Confederazione Svizzera
Confederaziun svizra

Swiss Confederation

Federal Department of Economic Affairs, Education and Research EAER
State Secretariat for Education, Research and Innovation SERI

Document information Table

Project Data			
Project Acronym	FLOW		
Project Title	Flexible energy system Leveraging the Optimal integration of EVs deployment Wave		
Grant Agreement n.	101056730		
Topic identifier	HORIZON-CL5-2021-D5-01-03		
Funding Scheme	RIA		
Project duration	48 months		
Coordinator	Catalonia Institute for Energy Research		
Website	https://www.theflowproject.eu/		
Deliverable Document Sheet			
Deliverable No.	4.3		
Deliverable title	Advanced flexibility management system description and functionalities		
Description	Describes the EMS improvements implemented to enable V2X functionality and improve energy system performance		
WP No.	4		
Related task	4.3		
Lead beneficiary	RSE		
Author(s)	Giuseppe Silano (RSE), Tomas Montes (IREC), Ferran Pinsach (IREC), Lucía Igualada (IREC), Josh Eichman (IREC), István Bara (TUD), and Gautham Ram Chandra Mouli (TUD)		
Contributor(s)	RSE, IREC, TUD		
Type	Report		
Dissemination L.	Public		
Due Date	31/12/2023	Submission Date	14/12/2023

Funded by the European Union

Version	Date	Author(s)	Organization(s)	Comments
V0.1	29/08/2023	Giuseppe Silano	RSE	Create the document and highlight the key points
V0.2	15/10/2023	Giuseppe Silano, Tomas Montes, Ferran Pinsach, Lucía Igualada, Josh Eichman, István Bara, and Gautham Ram Chandra Mouli	RSE, IREC, TUD	Comments, discussions, and revision of the document with modifications to the various sections
V0.5	30/10/2023	Giuseppe Silano	RSE	Progressed and competition of initial draft for revision
V0.7	15/11/2023	Madlen Günther, Bettina Kämpfe, Ferdinando Bosco	TUC, ENG	Received reviewers' comments
V0.9	30/11/2023	Giuseppe Silano	RSE	Modified the draft following the review comments and performed the format setting
V1.0	14/12/2023	Josh Eichman, Sarah Cnockaert	IREC	Revising all sections and final submission on the EU portal

Funded by the European Union

DISCLAIMER

Funded by the European Union (EU). Views and opinions expressed are however those of the author(s) only and do not necessarily reflect those of the EU or CINEA. Neither the EU nor the granting authority can be held responsible for them.

Funded by the European Union

Table of contents

Funded by the European Union

Funded by the European Union

List of Tables

Funded by the European Union

List of Figures

Funded by the European Union

List of Acronyms

Acronym	Meaning
AI	Artificial Intelligence
BESS	Battery Energy Storage Systems
BMS	Battery Management System
ASM	Ancillary Service Market
CC-CV	Constant Current-Constant Voltage
CPO	Charging Point Operators
CSO	Charger Station Operator
C-rate	Charge-discharge rate
DAM	Day-Ahead Market
DC	Direct Current
DoD	Depth of Discharge
DP	Dynamic Process
DSO	Distribution System Operator
EV	Electric Vehicle
EMS	Energy Management System
FC	Free Charge
FEC	Full Equivalent Cycle
GEV	Gridable Electric Vehicle
LFP	Lithium Ferrum Phoshpate
MCDM	Multi-Criteria Decision-Making
MILP	Mixed-Integer Linear Program
MOA	Multi Objective Algorithms
MOIP	Multi-Objective Integer Programming
mSoC	Mean State of Charge
NCA	Nickel Cobalt Aluminum
NMC	Nickel Manganese Cobalt
OSCD	Orchestrating Smart Charging in-mass Deployment
PC	Paid Charge
SoC	State of Charge
SoH	State of Health
SPLOM	ScatterPLOt Matrix
TC	Total Cost
TCR	Total Cost Reduction
ToU	Time of Use
TT	Time of Use Tariff
TSO	Transmission System Operator
V1G	Unidirectional power flow
V2G	Vehicle-to-Grid
V2H	Vehicle-to-Home
V2V	Vehicle-to-Vehicle
V2X	Vehicle-to-Everything
WP	Work Package

Funded by the European Union

Executive Summary

Expanding Electric Vehicle (EV) charging functionality to include Vehicle-to-Everything (V2X) requires improvements to existing Energy Management Systems (EMSs). These systems should account for the development of advanced optimization algorithms that are scalable for mass deployment and capable of co-optimizing across multiple objectives including grid needs, user needs, and other connected resources like microgrids and distributed energy resources while factoring in the constraints from the vehicle and the charging infrastructure. Furthermore, the so-formulated EMSs should internalize the impacts on the life of the battery and power electronics to understand its effect on the decision-making process for V2X. Additionally, these advanced EMSs should be capable of combining Artificial Intelligence (AI) forecast modules with optimization modules and offering optimal management and flexibility services at different time horizons (e.g., real-time, 5 min, 15 min, 24h) to serve different grid needs.

Deliverable D4.3 “Advanced flexibility management system description and functionalities” is among the deliverables (i.e., D4.1, D4.2, D4.4, and D4.5) of Work Package 4 (WP4) describing the EMS improvements implemented to enable V2X functionality and enhance energy system performance within the FLOW project.

Based on this description, task T4.3 focuses on designing advanced smart charging solutions to successfully integrate EVs into electric power systems by combining AI modules developed in task T4.2 and leveraging the requirements and motivations identified in WP1. Task T4.3 contributes to the FLOW Objectives “Define, improve and validate a portfolio of EV smart charging configurations, technologies, and strategies for a range of applications and use cases.” This contribution is achieved through two main case studies: one involving a private parking lot and another involving two medium and medium and large-sized public parking lots. Hence, the main purpose of this document is to describe the research effort and results obtained within task T4.3 between months M4-M18 of the project. The main contributions of this deliverable can be summarized as follows:

- Presenting concise summaries of key concepts that serve as the groundwork for the content in deliverable D4.3 and the activities conducted within the task T4.3. These explanations aim to underscore the paramount importance of V2X technology, illuminate the intricacies of EMS, and outline the cutting-edge areas of focus in EMS research. Among these forefront considerations, EMS approaches that account for uncertainties, delve into battery degradation models, and tackle the complexities of multi-criteria optimization challenges are also examined. These insights collectively provide a comprehensive foundation, paving the way for the detailed investigations that ensure power system stability, and effectively orchestrating EV fleet participation in grid operations.
- Quantifying the economic benefits associated with the provision of ancillary services to the grid. The analysis is based on a recent Vehicle-to-Grid (V2G) energy management framework introduced by RSE (Vignali, Falsone, Ruiz, & Gruosso, 2022), while its methodology can be applied to alternative V2G frameworks. The analysis defines necessary and sufficient conditions for profitability and illustrates through numerical simulations using MATLAB.
- Developing of a highly flexible multi-objective optimization algorithm and establishing a foundational EMS for the scheduling of EV charging. This challenge is addressed through a Mixed-Integer Linear Program (MILP) formulation inspired by previous work of the TUD (Mouli,

Funded by the European Union

Kefayati, Baldick, & Bauer, 2019). Numerical simulations in JuMP[1] (Lubin, et al., 2023) using Gurobi[2] as the solver vividly showcases the adaptability of the algorithm while highlighting the pivotal role of the multi-objective approach.

- Characterizing the strengths and weaknesses of the most referenced EMSs for EV charging, with a particular focus on areas for potential improvement and strategies to encourage the adoption of battery degradation models in charging methods. This effort aims to emphasize the importance of considering degradation as a crucial element of charge management.

The remainder of the document is structured as follows. Section 1 presents a concise summary of key concepts that serve as the groundwork for the content in deliverable D4.3 and the activities conducted within the task T4.3. Section 2 quantifies the economic benefits associated with the provision of ancillary services to the grid. Section 3 presents a highly adaptable multi-objective optimization algorithm and a foundational EMS for EV charging scheduling. Section 4 discusses the strengths and weaknesses of EVs, emphasizing the potential of integrating battery degradation models and their role in reducing the total cost of charging and mitigating environmental impact by extending the EV's battery life. Finally, conclusions are drawn in Section 5.

[1] https://jump.dev/JuMP.jl/stable/
[2] https://www.gurobi.com/

Funded by the European Union

1. EMS to enable V2X functionality

In the upcoming sections, we will provide concise summaries of pivotal concepts that lay the foundation for the contents of this deliverable and the work conducted within task T4.3. These elucidations are designed to highlight the paramount significance of Vehicle-To-Everything (V2X) technology, shed light on the complexities of Energy Management Systems (EMSs), and outline the cutting-edge focal points within the realm of EMS exploration. Among the forefront considerations, we will delve into the realm of EMS that considers uncertainties, explore battery degradation models, and navigate the complexities of multi-criteria optimization challenges. These insights will collectively offer a comprehensive overview, setting the stage for the detailed explorations that follow.

1.1. The need for an EMS

In the realm of advancing environmental concerns and clean energy priorities, Electric Vehicles (EVs) have garnered increasing attention from governments, industries, and consumers alike. Recognized as a potent strategy to diminish oil dependency, curb gas emissions, and amplify energy conversion efficiency, EVs have sparked a transformative revolution in the automotive market (Chan, 2007), (Williams, et al., 2012). Previous years have seen concentrated efforts on refining EV components, ranging from electric machines and drive systems to batteries, fuel cells, and onboard renewable energy sources (Sovacool & Hirsh, Beyond batteries: an examination of the benefits and barriers to plug-in hybrid electric vehicles (PHEVs) and a vehicle-to-grid (V2G) transition, 2009). Yet, with the emergence of the smart grid paradigm, EVs are primed to assume a fresh role enabling energy exchange with the power grid. The surge in electric mobility has witnessed a remarkable upswing in the global electric car fleet, surpassing 7.2 million units in 2019 with a 40% annual rise. This upward trajectory persisted into 2020, culminating in over 10 million EVs worldwide (Association, 2023).

Despite to the promising trajectory of EV adoption, the cumulative energy demands posed by a substantial EV fleet could potentially strain energy supply systems. The resultant challenges span voltage regulation, peak-load demands, frequency fluctuations, and harmonic contamination. Herein, the implementation of a smart grid system assumes paramount significance, handling the integration of EVs and fleet planning to minimize power system stress. Smart EV charging systems can optimize electricity demand patterns, thus mitigating power system strain. The concept of V2G technology gains importance, where EV batteries function as energy storage units capable of contributing power back to the grid during peak-load demands (Sovacool, Axsen, & Kempton, Tempering the Promise of Electric Mobility? A Sociotechnical Review and Research Agenda for Vehicle-Grid Integration (VGI) and Vehicle-to-Grid (V2G), 2017).

These grids connected EVs, denoted as Gridable EVs (GEVs), possess the capability not only to draw energy from the power grid through plug-in functionality but also to feed energy back into the grid using bidirectional chargers. This is facilitated by the presence of Direct Current (DC) link capacitors within the bidirectional chargers, inherently equipped to supply reactive power support to the power grid. In contrast to traditional fossil fuel power plants, which exhibit overall efficiency of approximately 30%, renewable energy sources boast remarkable efficiency levels of about 70% from generation to grid connection (Pecas Lopes, Joel Soares, & Rocha Almeida, 2010).

Funded by the European Union

Capitalizing on the charging and discharging capabilities of GEVs, coupled with the energy-efficient mandates of the power grid, the concepts of Vehicle-to-Home (V2H), Vehicle-to-Vehicle (V2V), Vehicle-to-Grid (V2G), and more in general V2X, have gained increasing attention in recent times. These concepts empower GEVs to transcend their roles as mere transportation tools, instead functioning as manageable loads and distributed sources for the power grid. Consequently, GEVs can act positive influence across home, community, and distribution grids during their charging and discharging cycles. Concurrently, the associated bidirectional chargers can inject reactive power into the grid via capacitors, significantly contributing to grid stability (Liu C. , Chau, Wu, & Gao, 2018), (Prencipe, van Essen, Caggiani, Ottomanelli, & Homem de Almeida Correia, 2022).

Hence, considering the manifold advantages and challenges connected with the expanding EV landscape, the need for an advanced EMS arises. An EMS serves as the system that effectively harmonizes the interplay of EVs, smart grids, and energy demand patterns. By optimizing the utilization of available energy resources, minimizing system stress, and strategically engaging with grid dynamics, an EMS emerges as the key to unlocking the full potential of this evolving energy ecosystem.

1.2. Essential EMS concepts

This section introduces the intricacies of EMS as it pertains to Deliverable D4.3. It provides insights on the challenges brought about by uncertainty in the context of EV fleet aggregation for grid services. We explore the source of uncertainties in EMS related to variables such as individual vehicle arrival and departure times, as well as their initial State of Charge (SoC). Additionally, we introduce the vital concepts of single and multi-objective optimization and discuss their significance in the domain of EV charging scheduling. We also delve into the limitations of single-objective optimization, which primarily revolves around cost minimization, and stress the importance of adopting multi-objective approaches to address conflicting objectives involving various stakeholders. Finally, considering the extensive discussion on battery degradation's impact on EV charging optimization, we will also touch upon how this factor introduces an additional layer of complexity into EMS strategies, further highlighting the need for advanced optimization approaches.

1.2.1. EMS under uncertainty

In the context of designing aggregation strategies to address EV fleet requirements, a central challenge arises from managing the inherent uncertainty associated with fleet behavior. This uncertainty encompasses several critical parameters, including the arrival and departure times of individual vehicles, as well as their initial SoC. These parameters are essential for the aggregator to effectively schedule power flows in line with fleet dynamics. Furthermore, when engaging in wholesale markets, the aggregator must navigate the unpredictable outcomes of ancillary services, adding another layer of uncertainty to the equation (Sriyakul & Jermsittiparsert, 2020).

As electrified transportation evolves, diverse approaches for aggregating EV fleets through direct control mechanisms have been proposed. These approaches vary based on the optimization objectives, operational timelines, and strategies for addressing uncertainty. Existing methodologies include deterministic models for day-ahead energy optimization, stochastic programming, scenario generation, and robust optimization (Liu & Etemadi, 2018), (DeForest, MacDonald, & Black, 2018), (Alipour, Mohammad-Ivatloo, Moradi-Dalvand, & Zare, 2017).

Funded by the European Union

Stochastic optimization techniques aim to maximize the expected profit of the aggregator while imposing constraints to limit the probability of noncompliance. These methods consider uncertainties in market prices, vehicle availability, reserves activation, energy prices, and renewable source generation. They encompass a broad spectrum of scenarios, ranging from power system constraints to participation in ancillary service markets (Sun, Neumann, & Harrison, 2020), (Shi, Li, Zhang, & Lee, 2020), (Porras, Fernández-Blanco, Morales, & Pineda, 2020).

Robust optimization, on the other hand, tackles uncertainty by formulating the worst-case scenario. This approach focuses on ensuring feasible solutions that withstand deviations caused by uncertainty. While robust formulations often concentrate on day-ahead planning of charging and discharging profiles, they sometimes exclude the integration of ancillary services in the aggregator's operations.

While both stochastic and robust optimization techniques offer valuable insights, they come with their challenges. Stochastic optimization necessitates detailed probability distribution information for uncertain variables and can lead to computationally intensive solutions. Moreover, it might not guarantee compliance with Transmission System Operator (TSO) requirements across all possible scenarios. Robust formulations, on the other hand, often prioritize charging/discharging profile planning without incorporating ancillary services (Vignali, Falsone, Ruiz, & Gruosso, 2022). Given these intricate dynamics, the presence of uncertainty underscores the imperative for a sophisticated EMS. An EMS plays a pivotal role in accounting for uncertainty, optimizing resource utilization, ensuring power system stability, and effectively orchestrating EV fleet participation in grid operations. By embracing uncertainty and incorporating strategies to mitigate its impact, an EMS enhances the agility and resilience of the entire energy ecosystem, paving the way for a more sustainable and reliable electric mobility landscape.

1.2.2. Single and multi-objective optimization approaches

In the process of formulating an optimization problem to address EV fleet requirements, an essential consideration is defining the problem itself. This involves expressing the primary objectives of an optimization algorithm through one or more objective functions. In the context of single-objective optimization, there is only one function at play. While this function may encompass multiple operational objectives, it does not take into account their interrelationships.

In numerous studies, a singular objective often takes center stage, typically involving cost minimization or reward maximization. While a cost function may encompass various components (e.g., electricity cost, battery degradation cost, etc.), this approach has its limitations. Certain objectives may clash with others, making it challenging to identify trade-offs using solely a cost-based formulation. Furthermore, this approach tends to focus on the perspective of a single actor (be it the EV user, TSO, DSO, etc.), without delving into the potential conflicts of interest among these stakeholders.

In the case of multi-objective optimization, two or more conflicting objectives are defined. There are multiple possible classifications for these problems. One of the most popular ones is based on the decision-making process (Cohon & Marks, 1975), (Chiandussi, Codegone, Ferrero, & Varesio, 2012):

- *A priori* methods where preferences information is available before the solution process;
- *A posteriori* methods where first possible (Pareto-optimal) solutions are identified, and then the decision-making process chooses one of the solutions;

Funded by the European Union

- Progressive methods where the generated solutions are iteratively refined based on the decision-maker's preferences.

Although limited in number, multi-objective EV charging scheduling approaches can also be found in the literature. Both *a prioiri* and a *posterioiri* methods have been investigated. In the former case, the multi-objective problem is always transformed into one or more single-objective formulations. The weighted sum method (e.g., (Garcia-Villalobos J. , Zamora, Knezovic, & Marinelli, 2016), (Singh, Das, Wen, Singh, & Thakur, 2023)), (Kapoor, Gangwar, Sharma, & Mohapatra, 2020) and hierarchical optimization (e.g., (Kaur, Singh, & Kumar, 2019), (Chung, Li, Yuen, Wen, & Crespi, 2019), (Jiang, Zhang, Li, Zhang, & Huang, 2017)) are two commonly used approaches, but these only provide one Pareto-optimal solution and do not represent the whole front.

Posterioiri methods include mathematical programming, metaheuristic algorithms and machine learning. Their common point is that they generate multiple nondominated solutions, which represent part of or the whole Pareto-front. With mathematical programming, different scalarizations are formed and then solved using single-objective optimization. Metaheuristic algorithms approximate the front in a single run, but the optimality cannot be guaranteed (Ruzika & Wiecek, 2005), (Coello Coello, Lamont, & Van Veldhuizen, 2007). The number of papers dealing with EV scheduling based on a posteriori methods is relatively small, but metaheuristic approaches seem more prevalent (Mishra, Mondal, & Mondal, 2022), (Einaddin & Yazdankhah, 2020), (Ahmadi, Arias, Hoogsteen, & Hurink, 2022), (Kharra, Tiwari, Singh, & Rawat, 2023), (Singh & Tiwari, Multi-Objective Optimal Scheduling of Electric Vehicles in Distribution System, 2018). Among the scalarization methods, the ε-constraint or augmented ε-constraint methods are the most often used (Maigha & Crow, 2018), (Zakariazadeh, Jadid, & Siano, 2014). While undoubtedly, cost will remain the most important aspect for the operator of the EMS, a holistic view of the possible objectives and their corresponding trade-offs is essential for the harmonic co-operation between the grid and EMS and for the provision of ancillary services. Conflicting objectives can only be handled effectively with a proper representation of the Pareto front. Thus, an *a posterioiri* multi-objective-based optimization is crucial for advanced EMSs.

1.2.3. Battery degradation's impact on EMS

Incorporating considerations related to battery degradation into EMS strategies presents a significant opportunity. Robust evidence suggests that battery usage patterns have a substantial impact on battery degradation, influencing factors such as reduced driving range and the total cost of ownership of EVs (Baure & Dubarry, 2020), (Jafari, Gauchia, Zhao, Zhang, & Gauchia, 2018). The limited adoption of battery degradation in charge optimization strategies is not indicative of its importance but is primarily due to its inherent complexity. Battery degradation is influenced by a multitude of factors, including temperature, Depth of Discharge (DoD), SoC, Charge-discharge rate (C-rate), ampere-hour throughput, cycle number, and storage duration, exhibiting nonlinear relationships among these variables.

While including battery degradation in the optimization of charging vehicles is not commonplace, it is a common practice in the field of stationary Battery Energy Storage Systems (BESS). Ignoring battery degradation in BESS optimization management controls can result in a lack of assurance for battery amortization (Xu, Oudalov, Ulbig, Andersson, & Kirschen, 2018), (García-Miguel, Alonso-Martínez, Arnaltes Gómez, García Plaza, & Asensio, 2022), (Rosewater, Copp, Nguyen, Byrne, & Santoso, 2019). The simplest approach to include degradation in optimization considers that battery lifetime is

Funded by the European Union

primarily influenced by the number of cycles or kWh throughput (Martins, Hesse, Jungbauer, Vorbuchner, & Musilek, 2018), (Saez-de-Ibarra, Martinez-Laserna, Stroe, Swierczynski, & Rodriguez, 2016). To enhance the accuracy of this degradation estimation, other factors such as SoC and C-rate can also be considered (Bai, Wang, & He, 2022), (Maheshwari, Paterakis, Santarelli, & Gibescu, 2020). While using degradation models offers benefits, the inherent nonlinearity of these models and the challenges associated with precisely incorporating factors like DoD contribute to the complexity of integrating them into an optimization problem (Zhao & Li, 2023).

In the realm of EVs, battery degradation consideration has traditionally centered on the driving phase, as demonstrated in (Wang, Jiao, & Sun, Energy Management Strategy in Consideration of Battery Health for PHEV via Stochastic control and Particle Swarm Optimization Algorithm, 2017). However, the concept of bidirectional power flow, such V2G, has gained significant attention as a potential source of multiple revenue streams and an opportunity to support grid operations (e.g., balancing, congestion). A substantial portion of optimization studies now focuses on assessing the degradation effects of discharging the battery when the vehicle is connected to a bidirectional charger, as exemplified by (Leippi, Fleschutz, & Murphy, 2022), (Thomposon, 2018). The problem formulation, akin to BESS optimization, incorporates additional features specific to charger technology, such as arrival time, departure time, and initial and final SoC. Some degradation factors, including cycles or kWh throughput (Singh & Tiwari, Cost Benefit Analysis for V2G Implementation of Electric Vehicles in Distribution System, 2020), SoC (Ahmadian, et al., 2018), and C-rate (Recalde Melo, Trippe, Gooi, & Massier, 2018), have been integrated into V2G management strategies. Moreover, power, SoC, and a simplified calculation of DoD were incorporated into models proposed by (Mal, Chattopadhyay, & Yang, 2013). More comprehensive degradation modelling has been explored using two-step optimization (Farzin, Fotuhi-Firuzabad, & Moeini-Aghtaie, 2016) or multi-objective models (Chung, Jangra, Lai, & Lin, 2020). Additionally, some studies have gone beyond merely considering electricity prices (Das, et al., 2020) and have included considerations for theoretical CO2 emissions during the charging process.

Despite extensive research on battery degradation in the context of V2G applications, unidirectional chargers, which are currently the predominant charger type, have received limited attention. Much of the literature often explores battery considerations across various charging methods (Bandara, Viera, & González, 2022). However, concerning optimal economic management, the integration of degradation stress factors into the optimization model remains relatively limited. For instance, (Wei, Li, & Cai, 2018) optimizes EV charging while incorporating degradation as a power function.

The complexity of battery models and the challenges associated with their integration into EV charge optimization models, coupled with the diversity of battery technologies across EVs, pose significant challenges for Charger Station Operators (CSOs). Furthermore, commonly used communication protocols between vehicles and chargers, such as ISO 15118[3] or IEC 61851[4], lack sufficient information to incorporate degradation effects into optimization models, resulting in both theoretical and practical limitations.

[3] https://www.iso.org/standard/77845.html
[4] https://www.iecee.org/certification/iec-standards/iec-61851-242014

Funded by the European Union

2. V2G and Ancillary Services: A profitability analysis under uncertainties

This section deals with briefly presenting the research effort conducted in task T4.3 by adding a further level of technical detail those foreseen in the Executive Summary. The activity ended up with a profitability analysis (Bianchi, Falsone, & Vignali, 2023) with reference to an early framework for V2G optimal operation in presence of uncertainty (Vignali, Falsone, Ruiz, & Gruosso, 2022). The analysis provides necessary and sufficient conditions for profitability in a simplified case. Numerical simulations in MATLAB showcase the validity and effectiveness of the analysis and that it also holds for a more general case.

2.1. Introduction

EVs sales continue to break records as nearly 10% of global car sales were electric in 2021, four times the market share in 2019[5]. This rapid and significant spread of EVs plays a fundamental role in the energy transition. In addition to the new challenges associated with charging needs, the introduction of EVs represents a new opportunity, thanks to the possible provision of ancillary services. Indeed, the modulation of the charging power, and even the discharge of the vehicles, enable the provision of services to the electricity network (Liu C. , Chau, Wu, & Gao, 2013). However, since an individual EV's energy capacity is limited, EVs need to be grouped by means of EV aggregators to form a flexible load with enough energy content for grid operations. Once the fleet is formed, the aggregator must coordinate the actions of the EV pool to participate in electricity markets, guaranteeing compliance with traded consumption plans and services (Bessa & Matos, 2012).

The optimal dispatch of the charging power of each vehicle is usually formulated as an optimization problem, in which the aggregator aims to maximize its revenues from the provision of services, minimizing at the same time the EVs charging costs while satisfying the requests of the EV owners, e.g., minimum charging level at departure. Solving this problem needs to account for several factors: aggregator business model, technical limitations of vehicles and aggregator, availability of vehicles, market outcomes. Realistic formulations of this problem necessarily involve considering uncertainty in the fleet behavior and energy markets. Specifically, it is necessary to model the random presence of vehicles, the initial uncertain SoC with which the vehicles start parking and the actual service signal provided by the Transmission System Operator (TSO). Several techniques have been proposed in the last two decades for solving this optimization problem, which differ on how uncertainty is handled and the modelling choices for the discussed factors (Garcia-Villalobos J. , Zamora, SAn Martin, Asensio, & Aperribay, 2014), (Tan & Ramachandaramurthy, 2016), (Nimalsiri, Mediwaththe, Ratnam, Shaw, & Halgamuge, 2019), for a comprehensive review on different strategies.

In many of these works, costs-benefits analysis related to the provision of ancillary services have been made experimentally by, e.g., varying energy market prices and battery degradation costs, from the point of view of both EV owners and aggregators (Sortomme & El-Sharkawi, 2011), (De Los Rıos, Goentzel, Nordstrom, & Siegert, 2012), (Calvillo, Czechowski, Soder, Sanchez-Miralles, & Villar, 2016).

[5] https://www.iea.org/reports/global-ev-outlook-2022

Funded by the European Union

However, the size of the benefits varies significantly due to varying modelling approaches, different assumptions, considered applications, countries, and vehicle types, often leading to inconsistent and contradictory results (Heilmann & Friedl, 2021). Also, to the best of authors' knowledge, no-one provided an overall picture describing profitability conditions for offering balancing services. For example, one may be interested in assessing which should be the expected profit of an upward service in relation to the per unit energy cost used for charging the vehicle, to make this kind of service profitable. Clearly, answering to this question requires to account for the (uncertain) TSO signal, both in the modelling framework and in the costs-benefits analysis. This kind of analysis helps in incentivizing the participation of EVs' owners in the mentioned aggregation scheme, thus contributing to the transition that the energy sector is facing which asks for additional sources of flexibility to guarantee reliable grid operation.

Recently, a first attempt towards a comprehensive framework for optimal dispatching in presence of uncertainty has been made in (Vignali, Falsone, Ruiz, & Gruosso, 2022). The authors considered all the three sources of uncertainty discussed above, adopting a robust paradigm to enforce the constraints and an expectation paradigm for the cost function. However, they did not analyze the profitability of providing ancillary services. In this section, we build upon the framework introduced by (Vignali, Falsone, Ruiz, & Gruosso, 2022), and we provide necessary and sufficient conditions for the profitability of offering upward and downward balancing services. Specifically, we provide analytic conditions in a simplified case, and we show via simulation that they also hold for the general case. Based on these conditions, we also provide insights on how to make ancillary services more profitable by considering the possibility of participating also to intraday energy markets besides the day-ahead and ancillary service markets, to compensate for the effects of the actual provision of services during the day.

2.2. Preliminaries

Let us first briefly recall the framework introduced in (Vignali, Falsone, Ruiz, & Gruosso, 2022) and introduce two common scenarios we will consider in the profitability analysis.

2.2.1. Framework

In reference to an aggregator of EVs, as discussed reference in (Vignali, Falsone, Ruiz, & Gruosso, 2022) this study addresses the finite horizon optimal control problem. The objective is to plan the power exchange profile for the next day and determine the maximum amount of upward and downward power variations that the EV fleet can supply to the main grid. The aim is to minimize EV charging costs and maximize the revenues derived from providing ancillary services.

To this end, the considered one-day time horizon is discretized into T time intervals (referred to as timeslots) indexed by $k = \{0, \dots, T-1\}$, each of duration τ. The introduced framework is very general and considers several sources of uncertainty like the first a_i and last d_i timeslots EV i is connected, the i-th battery energy content at EV arrival e_i^0, and the TSO service signal $\omega_k \in [-1, 1]$ modelling if and how much of the offered upward/downward services will be requested by the TSO. These are all random quantities as they are not known during day-ahead planning.

2.2.2. Notation

To improve readability, a summary of the notation used within this section is provided in the following.

Funded by the European Union

T, k, τ	Time intervals, time index, and time interval duration
$c^{dam}, c^{asm}, c^{veh}$	Cost to buy energy on the day-ahead (c^{dam}) and ancillary service (c^{asm}) markets, and revenue (c^{veh}) paid to the owner of the vehicle
$p_{k,i}^{dam}, p_{k,i}^{asm}$	Power bought on the day-ahead ($p_{k,i}^{dam}$) and ancillary service ($p_{k,i}^{asm}$) markets at time slot k for the i-th EV
a_i, d_i	Arrival and departure times of the i-th EV
$[\cdot]^+, [\cdot]^-, K_{k,s,i}$	Short form for $[\cdot]^+ = \max\{\cdot, 0\}$ and $[\cdot]^- = [\cdot]^+$, and disturbance feedback term
$c^{s+}, c^{s-}, c^{e+}, c^{e-}, c^{v+}, c^{v-}$	Cost to buy (c^{s+}) and sell (c^{s-}) energy on the ancillary service and the day-ahead markets (c^{e+} and c^{e-}) for the aggregator, cost per paid by the owner of the vehicle to buy (c^{v+}) and sell (c^{v-}) energy
$\omega_k, s_{k,i}^+, s_{k,i}^-, \omega_s$	Uncertain service signal, maximum up ($s_{k,i}^+$) and down ($s_{k,i}^-$) power variation offered by the i-th EV at the time slot k, and TSO service signal
$e_i^o, e_{k,i}, e_i^{min}, e_i^{max}, e_{d_i}, e^-, e^+, e_0$	Initial energy content, energy content at the time slot k, minimum energy content, maximum energy content, energy at the departure of the i-th EV
$\alpha_i, \eta_{k,i}, \eta_i^+, \eta_i^-$	Self-discharging losses, charging/discharging losses, charging losses, and discharging losses
$\Delta_e^o, \Delta_e^{max}$	Short notation for $e^o - e_0$ and $\Delta_e^{max} - e^+$
e^{dam}, e^{asm} e^{max}, e^{min}	Energy provision on the day-ahead and ancillary service markets for the aggregator Maximum and minimum values of the energy provision for the aggregator
$p_{k,i}, p_i^{min}, p_i^{max}, p^{min}, p^{max}$	Average charging power, minimum charging power, and maximum charging power of the i-th EV Minimum and maximum charging power of the aggregator
δ	Symbol used for identifying the uncertain parameters,
$\tilde{e}^{dam}, \tilde{e}^{asm}$	Expected provision on the day-ahead and ancillary service markets
$J_{FC}^o, J_{FC}^{asm}, J_{FC}^{\Delta}, J_{PC}^{o}, J_{PC}^{asm}, J_{PC}^{\Delta}$	Cost functions in the free charge and paid charge cases

2.2.3. EV modelling

In (Vignali, Falsone, Ruiz, & Gruosso, 2022) each EV is modelled as a battery

$$e_{k+1,i} = \alpha_i e_{k,i} + \tau\, \eta_{k,i}\, p_{k,i}, \qquad k \in [a_i, d_i], \tag{2.1}$$

Funded by the European Union

where $e_{k,i}$ is the energy content at the beginning of the time slot k, $p_{k,i}$ denotes the average charging ($p_{k,i} > 0$) or ($p_{k,i} < 0$) power during the timeslot k, $\alpha_i \in (0,1]$ models self-discharging losses, and

$$\eta_{k,i} = \begin{cases} \eta_i^+, & p_{k,i} \geq 0 \\ \dfrac{1}{\eta_i^-}, & p_{k,i} < 0 \end{cases}, \qquad 2.2$$

models charging/discharging losses, $\eta_i^+, \eta_i^- \in (0,1]$ being the charging/discharging efficiencies. The battery energy content $e_{k,i}$ always stays within a minimum $e_i^{min} > 0$ and maximum $e_i^{max} > 0$ and therefore

$$e_i^{min} \leq e_{k,i} \leq e_i^{max}, \qquad 2.3$$

must hold for any timeslot $k \in [a_i, d_i]$ in which the i-th EV is connected to the charging station. Similarly, individual, and aggregate power exchange are constrained as

$$\begin{aligned} p_{k,i} &\in [-p_i^{max}, p_i^{max}], & k &\in [a_i, d_i] \\ p_{k,i} &= 0, & k &\notin [a_i, d_i] \end{aligned} \qquad 2.4$$

since each EV has a maximum power exchange p_i^{max} when connected and its power exchange must be zero when disconnected, and

$$-p^{max} \leq \sum_{i=1}^{N} p_{k,i} \leq p^{max}, \qquad 2.5$$

for all timeslots, as the charging stations are all connected to the same point of exchange with the grid, which can withstand a maximum power exchange equal to p^{max}. In most cases, a minimum battery energy content at departure is required by the user. This can be easily considered by enforcing the constraint

$$e_{d_i+1,i} \geq e_i^o, \qquad 2.6$$

where dove $e_i^o \in [e_i^{min}, e_i^{max}]$ is i-th EV desired energy at departure.

2.2.4. Cost terms

To charge the EVs, the aggregator must buy energy on the market, and it can do so both on the Day-Ahead Market (DAM) or on the Ancillary Services Market (ASM). Let $p_{k,i} = p_{k,i}^{dam} + p_{k,i}^{asm}$, $p_{k,i}^{dam}$ and $p_{k,i}^{asm}$ being the portion of power bought in DAM and in ASM, respectively. At any timeslot k, buying an energy unit on the DAM costs c_k^{e+} to the aggregator, while selling energy to the grid pays $c_k^{e-} < c_k^{e+}$per energy unit. The aggregator buys energy whenever the net power requested by all EVs is positive and sells energy otherwise. The cost incurred for the DAM over the entire horizon is thus given by

$$c^{dam} = \sum_{k=0}^{T-1} c_k^{e+} \left[\sum_{i=1}^{N} \tau p_{k,i}^{dam} \right]^+ - c_k^{e-} \left[\sum_{i=1}^{N} \tau p_{k,i}^{dam} \right]^-, \qquad 2.7$$

Funded by the European Union

where $[v]^+ = max\{v, 0\}$ denotes the positive part of its argument and $[v]^- = [-v]^+$ its negative part. As for the ancillary services, since they are typically divided into upward and downward services, it is convenient to express

$$p_{k,i}^{asm} = [\omega_k]^+ s_{k,i}^+ - [\omega_k]^- s_{k,i}^-, \tag{2.8}$$

where $s_{k,i}^+ \geq 0$ and $s_{k,i}^- \geq 0$ are the maximum power variations offered by i-th EV in timeslot k for the downward and upward services respectively, and ω_k is the uncertain service signal sent by the TSO.

An energy unit bought (as a downward service) on the ASM costs $c_k^{s+} < c_k^{e+}$, while an energy unit sold (as an upward service) pays $c_k^{s-} > c_k^{e+}$, leading to the following total cost incurred by the aggregator

$$c^{veh} = \sum_{k=0}^{T-1} c_k^{s+} \sum_{i=1}^{N} \tau [\omega_k]^+ s_{k,i}^+ - c_k^{s-} \sum_{i=1}^{N} \tau [\omega_k]^- s_{k,i}^-, \tag{2.9}$$

where the sign and magnitude of $\omega_k \in [-1, 1]$ determine whether an upward ($\omega_k < 0$) or downward ($\omega_k > 0$) will be requested by the TSO and by which extent, or if no service will be requested ($\omega_k = 0$), for each timeslot k.

Depending on the situation, the aggregator may want to charge/pay the EV owners for recharging/discharging their vehicles. In such cases, the aggregator will receive $c_k^{v+} > c_k^{e+}$ per energy unit used for charging an EV and will pay $c_k^{v+} > c_k^{v-}$ to the EV owner for each energy unit discharged[6], thus having the following additional cost term

$$c^{veh} = \sum_{k=0}^{T-1} \sum_{i=1}^{N} c_k^{v-} [\tau p_{k,i}]^- - c_k^{v+} [\tau p_{k,i}]^+. \tag{2.10}$$

2.2.5. Optimal planning

Unfortunately, an optimization problem involving the introduced constraints and cost terms would be ill-posed due to their dependency from the uncertain parameters a_i, d_i, e_i^0, and ω_k, collectively referred to as δ. The authors in (Vignali, Falsone, Ruiz, & Gruosso, 2022) proposes to adopt a robust paradigm to enforce the constraints and an expectation paradigm for the cost function. Accordingly, we will focus on the following problem

$$\begin{aligned} \min_{p_{k,i}^{dam}, s_{k,i}^+, s_{k,i}^-} \quad & c^{dam} + \mathbb{E}[c^{asm} + c^{veh}] & \\ s.t. \quad & eq. 2.5, & \forall k, \forall \delta \\ & eqs. 2.3, 2.4, 2.6, & \forall i, \forall \delta \\ & s_{k,i}^+, s_{k,i}^- \geq 0 & \forall i, \forall k \end{aligned}. \tag{2.11}$$

[6] Costs for battery degradation can be accounted for in c_k^{v-} (Hoke, Brissette, Smith, Pratt, & Maksimovic, 2014).

Funded by the European Union

More specifically, we will consider two business models: 1) *Free-Charge* (FC), without the c^{veh} term, representative of a company willing to provide the recharge service to its employees and, ii) *Paid Charge* (PC), with the c^{veh} term, in case EVs charging is the core business of the parking lot owner.

2.3. Profitability Analysis

We are interested in providing conditions under which the provision of ancillary services is profitable for an aggregator of EVs adopting either the Free Charge (FC) or Paid Charge (PC) business model introduced above. Numerical investigations, despite being informative, can hardly give an overall picture on profitability, as results are masked by the complexity of problem 2.11 and by the uncertainty affecting the simulation of optimal control policies. Therefore, in this section, we begin by simplifying the framework and subsequently derive precise necessary and sufficient conditions for achieving profitability.

2.3.1. Framework reduction

We impose the following simplifying assumptions. We consider the optimization of one vehicle ($N = 1$ and we drop the subscript i), as multiple vehicles can be considered, to some extent, a unique "big" vehicle. We set $\eta_k = \alpha = 1$ as they are typically close to unity. All costs are time-invariant (we drop the subscript k). Since the costs are time-invariant, we can consider a unique timeslot ($T = 1$) lasting $\tau = 24h$ and reduce the analysis to energy considerations. Since $T = 1$, we set $a_i = a = d_i = d = 0$, which are now deterministic. We consider only the TSO request $\omega_k = \omega$ as uncertain quantity since the initial energy $e_i^o = e_0 \in [e_{min}, e^o]$ is only affecting the constraints. Under these assumptions, we have

$$\begin{aligned} p &= p^{dam} + s^+[\omega]^+ - s^-[\omega]^-, \\ e_1 &= e_0 + \tau p = e_0 + \tau p^{dam} + \tau s^+[\omega]^+ - \tau s^-[\omega]^-, \end{aligned} \tag{2.12}$$

and

$$\begin{aligned} c^{dam} &= c^{e+}[\tau p^{dam}]^+ - c^{e-}[\tau p^{dam}]^- \\ c^{asm} &= c^{s+}[\omega]^+ \tau s^+ - c^{s-}[\omega]^- \tau s^- \\ c^{veh} &= c^{v-}[\tau p]^- - c^{v+}[\tau p]^+ \end{aligned}, \tag{2.13}$$

and the optimization problem 2.11 becomes

$$\begin{aligned} \min_{p_{k,i}^{dam},\, s_{k,i}^+,\, s_{k,i}^-} \quad & c^{dam} + \mathbb{E}[c^{asm} + c^{veh}] \\ s.t. \quad & e^{min} \le e^o \le e_0 + \tau p \le e^{max}, \quad \forall \omega \\ & -p^{max} \le p \le p^{max}, \quad \forall \omega \\ & s^+, s^- \ge 0 \end{aligned}. \tag{2.14}$$

Since we typically have $\tau p^{max} \gg e^{max}$ (over the entire horizon we can charge the EV fully), the power constraints are redundant, and we are left with only energy quantities in eq. 2.14. Let $e^{dam} = \tau p^{dam}$, $e^+ = \tau s^+$, and $e^- = \tau s^-$, the robust counterpart of $e^o \le e_0 + \tau p \le e^{max}$ for all ω affecting τp is given by

Funded by the European Union

$$\Delta_e^o + e^- \leq e^{dam} \leq \Delta_e^{max} - e^+, \tag{2.15}$$

where $\Delta_e^o = e^o - e_0$ e $\Delta_e^{max} = e^{max} - e_0$, and it implies $e^{dam} \geq 0$. Problem 2.11 can thus be further reduced to

$$\begin{matrix} \min\limits_{e^{dam},\, e^+,\, e^-} & c^{dam} + \mathbb{E}[c^{asm} + c^{veh}] \\ s.t. & \Delta_e^o + e^- \leq e^{dam} \leq \Delta_e^{max} - e^+ \end{matrix}. \tag{2.16}$$

Before analyzing 2.16 it is worth recalling some inequalities involving the unitary energy prices

$$\begin{matrix} c^{v-} > c^{v+} > c^{e+} > c^{e-}, \\ c^{s-} > c^{e+} > c^{s+}. \end{matrix} \tag{2.17}$$

2.3.2. Profitability conditions: free charge

Let us consider the FC case first, where the cost term c^{veh} is absent. To assess whether offering ancillary services is profitable or not, consider the optimal solution when such services are not offered. This entails solving the following optimization problem

$$\begin{matrix} \min\limits_{e^{dam} \geq 0} & c^{dam} \\ s.t. & \Delta_e^o \leq e^{dam} \leq \Delta_e^{max} \end{matrix}, \tag{2.18}$$

whose optimal solution is $e^{dam} = \Delta_e^o$ since $c^{dam} = c^{e+}\, e^{dam}$ due to $e^{dam} \geq 0$ and $c^{e+} > 0$. If we now introduce the ancillary service provision, we are back to the problem 2.16 without c^{veh}. Clearly, $e^{asm} = \Delta_e^o$ with $e^+ = 0$ and $e^- = 0$ is feasible for the problem 2.16 and yields the same cost

$$J_{FC}^o = c^{e+}[e^{dam}]^+ - c^{e-}[e^{dam}]^- = c^{e+} e^{dam} = c^{e+} \Delta_e^o, \tag{2.19}$$

the second and third equality being due to $e^{dam} = \Delta_e^o > 0$. Therefore, for the problem 2.16 without e^{veh} to have a different solution there must exist a triplet $\tilde{e}^{dam} = \Delta_e^o + v$, $e^+ \geq 0$ and $e^- \geq 0$ satisfying the constraints of the problem 2.16, i.e.,

$$\Delta_e^o + e^- \leq \Delta_e^o + v \leq \Delta_e^{max} - e^+, \tag{2.20}$$

and achieving a better cost. Constraint 2.20 together with non-negativity of e^+ and e^- implies the following chain of inequalities

$$0 \leq e^- \leq v \leq \Delta_e^{max} - \Delta_e^o - e^+ \leq \Delta_e^{max} - \Delta_e^o, \tag{2.21}$$

and the cost associated to the new solution is

$$\begin{aligned} J_{FC}^{asm} &= c^{e+}[\tilde{e}^{dam}]^+ - c^{e-}[\tilde{e}^{dam}]^- + c^{s+}\mathbb{E}^+ e^+ - c^{s-}\mathbb{E}^- e^- \\ &= c^{e+}\Delta_e^o + c^{e+} v + c^{s+}\mathbb{E}^+ e^+ - c^{s-}\mathbb{E}^- e^- \\ &= J_{FC}^0 + \underbrace{c^{e+} v + c^{s+}\mathbb{E}^+ e^+ - c^{s-}\mathbb{E}^- e^-}_{\hat{J}_{FC}^{\Delta}} \end{aligned}, \tag{2.22}$$

Funded by the European Union

where $\mathbb{E}^+ = \mathbb{E}[[\omega]^+]$ and $\mathbb{E}^- = \mathbb{E}[[\omega]^-]$, the second equality is due to $\tilde{e}^{dam} = \Delta_e^o + v \geq 0$ since $v \geq 0$ by eq. 2.21, and the last equality is by definition of J_{FC}^o. We thus need to analyze the sign of J_{FC}^{Δ}. For any triplet (v, e^+, e^-) satisfying eq. 2.21, we have

$$\begin{aligned} J_{FC}^{\Delta} &= c^{e+}v + c^{s+}\mathbb{E}^+e^+ - c^{s-}\mathbb{E}^-e^- \\ &\geq c^{e+}v - c^{s-}\mathbb{E}^-e^- \\ &\geq (c^{e+} - c^{s-}\mathbb{E}^-)e^- \\ &\geq \min\{0, (c^{e+} - c^{s-}\mathbb{E}^-)(\Delta_e^{max} - \Delta_e^o)\}, \end{aligned} \qquad 2.23$$

where the first inequality holds for any $e^+ \geq 0$ (with $e^+ \geq 0$ as edge-case), the second inequality holds for any $v \geq e^-$ (with $v = e^-$as edge-case), and the last inequality holds for any e^- such that $0 \leq e^- \leq \Delta_e^{max} - \Delta_e^o$, with $e^- = 0$ or $e^- = \Delta_e^{max} - \Delta_e^o$ as edge-cases, each one yielding the respective term inside the minimum. Since $\Delta_e^{max} - \Delta_e^o > 0$, then, recalling $\tilde{e}^{dam} = \Delta_e^o + v$, we have the following edge-cases:

$$\begin{cases} v = 0 \\ \tilde{e}^{asm} = \Delta_e^o \\ e^+ = 0 \\ e^- = 0 \\ J_{FC}^{\Delta} = 0 \end{cases} \quad \Leftrightarrow \quad c^{e+} > c^{s+}\mathbb{E}^-, \qquad 2.24$$

$$\begin{cases} v = \Delta_e^{max} - \Delta_e^o \\ \tilde{e}^{dam} = \Delta_e^{max} \\ e^+ = 0 \\ e^- = \Delta_e^{max} - \Delta_e^o \\ J_{FC}^{\Delta} < 0 \end{cases} \quad \Leftrightarrow \quad c^{e+} < c^{s-}\mathbb{E}^-. \qquad 2.25$$

Therefore, if $c^{e+} > c^{s-}\,\mathbb{E}^-$, then $J_{FC}^{\Delta} \geq 0$ for any feasible alternative solution, hence $e^{dam} = \Delta_e^o$ remains the optimal solution. Otherwise, if $c^{e+} < c^{s-}\,\mathbb{E}^-$, then choosing $\tilde{e}^{dam} = \Delta_e^o + v = \Delta_e^{max}$, $e^+ = 0$, and $e^- = \Delta_e^{max} - \Delta_e^o$ yields $J_{FC}^{\Delta} = (c^{e+} - c^{s-}\,\mathbb{E}^-)(\Delta_e^{max} - \Delta_e^o) < 0$ and offering (upward) services is profitable. Note that since $(c^{e+} - c^{s-}\,\mathbb{E}^-)(\Delta_e^{max} - \Delta_e^o) < J_{FC}^{\Delta}$ for any feasible solution, we have that $\tilde{e}^{dam} = \Delta_e^{max}$, $e^+ = 0$, and $e^- = \Delta_e^{max} - \Delta_e^o$ is actually the optimal solution of the problem 2.16 without c^{veh}, so offering downward services is never convenient and the obtained condition is both necessary and sufficient for profitability.

The condition is also intuitive as providing upward services is convenient only if their expected revenue $c^{s-}\,\mathbb{E}^-$ per unit is greater than the cost c^{e+} of buying an energy unit in the DAM. Note also how the optimal strategy is to offer as an upward service only the quantity $\Delta_e^{max} - \Delta_e^o = e^{max} - e^o$ as offering more energy does not guarantee to satisfy the final energy constraint $e_1 \geq e^o$.

2.3.3. Profitability conditions: paid charge

Let us now focus on the PC case. As before, consider first the optimal solution when services are not offered. This entails solving the problem

$$\begin{aligned} \min_{e^{dam} \geq 0} \quad & c^{dam} + c^{veh} \\ s.t. \quad & \Delta_e^o \leq e^{dam} \leq \Delta_e^{max}, \end{aligned} \qquad 2.26$$

Funded by the European Union

where c^{veh} is now a deterministic cost since $\tau p = e^{dam} > 0$ when $e^+ = e^- = 0$. Moreover, $c^{dam} + c^{veh} = (c^{e+} - c^{v+})\, e^{dam}$ and, since $c^{e+} - c^{v+} < 0$ by eq. 2.17, then the optimal solution of the problem 2.26 is $e^{dam} = \Delta^{max}$.

If we now introduce the ancillary service provision, we are back to the problem 2.16. Clearly, $e^{dam} = \Delta_e^{max}$ with $e^+ = 0$ and $e^- = 0$ is feasible for the problem 2.16 and yields the same cost

$$\begin{aligned} J_{PC}^{o} &= (c^{e+} - c^{v+})[e^{dam}]^+ - (c^{e-} - c^{v-})[e^{dam}]^- \\ &= (c^{e+} - c^{v+})e^{dam} = (c^{e+} - c^{v+})\Delta_e^{max}, \end{aligned} \qquad 2.27$$

equalities being due to $e^{dam} = \Delta_e^{max} > 0$. Therefore, for the problem 2.16 to have a different solution there must exist a triplet $\tilde{e}^{dam} = \Delta_e^{max} + v$, $e^+ \geq 0$ and $e^- \geq 0$ satisfying the constraint of the problem 2.16, i.e.,

$$\Delta_e^o + e^- \leq \Delta_e^{max} + v \leq \Delta_e^{max} - e^+, \qquad 2.28$$

and achieving a better cost. Constraint 2.16 together with non-negativity of e^+ and e^- implies the following chain of inequalities

$$-(\Delta_e^{max} - \Delta_e^o) \leq e^- - (\Delta_e^{max} - \Delta_e^o) \leq v \leq -e^+ \leq 0, \qquad 2.29$$

and the cost associated to the new solution is

$$\begin{aligned} J_{PC}^{asm} &= c^{e+}[\tilde{e}^{dam}]^+ - c^{e-}[\tilde{e}^{dam}]^- + c^{s+}\mathbb{E}^+e^+ - c^{s-}\mathbb{E}^-e^- \\ &\quad + c^{v-}\mathbb{E}[[\tilde{e}^{dam} + e^+[\omega]^+ - e^-[\omega]^-]^-] \\ &\quad - c^{v+}\mathbb{E}[[\tilde{e}^{dam} + e^+[\omega]^+ - e^-[\omega]^-]^+] \\ &= c^{e+}\Delta_e^{max} + c^{e+}v + c^{s+}\mathbb{E}^+e^+ - c^{s-}\mathbb{E}^-e^- \\ &\quad - c^{v+}\mathbb{E}[\Delta_e^{max} + v + e^+[\omega]^+ - e^-[\omega]^-] \\ &= (c^{e+} - c^{v+})\Delta_e^{max} + (c^{e+} - c^{v+})v \\ &\quad + (c^{s+} - c^{v+})\mathbb{E}^+e^+ + (c^{v+} - c^{s-})\mathbb{E}^-e^- \\ &= J_{PC}^{o} + \underbrace{(c^{e+} - c^{v+})v + (c^{s+} - c^{v+})\mathbb{E}^+e^+ + (c^{v+} - c^{s-})\mathbb{E}^-e^-}_{J_{PC}^{\Delta}} \end{aligned} \qquad 2.30$$

where the second equality is due to $\tilde{e}^{dam} = \Delta_e^{max} + v \geq 0$ since $v \geq -(\Delta_e^{max} - \Delta_e^o)$ by eq. 2.29 together with $\tilde{e}^{asm} + e^+ [\omega]^+ - e^- [\omega]^- \geq \Delta_e^{max} + v - e^- \geq \Delta_e^o$ by eq. 2.29, nonnegativity of e^+ and e^-, and the fact that $\omega \in [-1, 1]$. The third equality is due to linearity of the expected value operator and the last equality uses the definition of J_{PC}^o and $J_{PC}^{\Delta} = (c^{e+} - c^{v+})v + (c^{s+} - c^{v+})\mathbb{E}^+e^+ + (c^{v+} - s^-)\mathbb{E}^-e^-$. Similarly, to the FC case, we need to analyze the sign of J_{PC}^{Δ}.

To ease the notation, let $g^o = c^{v+} - c^{e+} > 0$, $g^+ = \mathbb{E}^+(c^{v+} - c^{s+}) > 0$, and $g^- = \mathbb{E}^-(c^{s-} - c^{v+}) > 0$, inequalities being due to eq. 2.17. For any triplet (v, e^+, e^-) satisfying eq. 2.29, we have

$$\begin{aligned} J_{PC}^{\Delta} &= -g^o v - g^+e^+ - g^-e^- \\ &\geq (g^+ - g^o)v - g^-e^- \\ &\geq \min\{0, (g^o - g^+)(\Delta_e^{max} - \Delta_e^{\circ}), -g^-(\Delta_e^{max} - \Delta_e^{o})\} \end{aligned} \qquad 2.31$$

Funded by the European Union

where the first inequality is due to $-e^+ \geq v$ (with $e^+ = -v$ as edge-case) and the second inequality is given by the fact that, due to $e^- \leq v + \Delta_e^{max} - \Delta_e^o$ with $v \leq 0$ and $e^- \geq 0$, we are left with three possible edge-cases: $v = e^- = 0$ or $v = -(\Delta_e^{max} - \Delta_e^o)$ and $e^- = 0$ or $v = 0$ and $e^- = \Delta_e^{max} - \Delta_e^o$, (with $e^+ = -v$ in all cases), each one yielding the respective term inside the minimum. Since $\Delta_e^{max} - \Delta_e^o > 0$, then, recalling $\tilde{e}^{dam} = \Delta_e^{max} + v$, we have the following edge-cases:

$$\begin{cases} v = 0 \\ \tilde{e}^{dam} = \Delta_e^{max} \\ e^+ = 0 \\ e^- = 0 \\ J_{PC}^{\Delta} = 0 \end{cases} \Leftrightarrow \begin{cases} g^+ - g^o < 0 \\ g^- < 0 \end{cases}, \tag{2.32}$$

$$\begin{cases} v = -(\Delta_e^{max} - \Delta_e^o) \\ \tilde{e}^{dam} = \Delta_e^{max} \\ e^+ = \Delta_e^{max} - \Delta_e^o \\ e^- = 0 \\ J_{PC}^{\Delta} < 0 \end{cases} \Leftrightarrow \begin{cases} g^+ - g^o > 0 \\ g^- < g^+ - g^o, \end{cases} \tag{2.33}$$

$$\begin{cases} v = 0 \\ \tilde{e}^{dam} = \Delta_e^{max} \\ e^+ = 0 \\ e^- = \Delta_e^{max} - \Delta_e^o \\ J_{PC}^{\Delta} < 0 \end{cases} \Leftrightarrow \begin{cases} g^- > 0 \\ g^- > g^+ - g^o. \end{cases} \tag{2.34}$$

Now let us notice that $g^o = c^{v+} - c^{e+}$ represents the marginal gain of buying an energy unit in the DAM and selling it to the vehicle, $g^+ = \mathbb{E}^+ (c^{v+} - c^{s+})$ represents the marginal gain of buying an energy unit in the ASM (downward service) and selling it to the vehicle, $g^- = \mathbb{E}^- (c^{s-} - c^{v+})$ represents the marginal gain of selling an energy unit in the ASM (upward service) instead of selling it to the vehicle (i.e., the actual (expected) gain in offering the upward service), and $g_0^+ = g^+ - g^o$ represents the marginal gain of buying an energy unit in the ASM (downward service) instead of in the DAM to sell to the vehicle (i.e., the actual (expected) gain in offering the downward service). Given the preceding observations, we need to focus on g_0^+ and g^- only, and the above optimality conditions becomes also intuitive.

Similarly, to the FC case, since each edge-case achieves the minimum of J_{PC}^{Δ} under the respective conditions on g^o, g^+, and g^-, we have that each edge-case is actually the optimal solution of the problem 2.16 under the corresponding conditions. Therefore, the above conditions on g^o, g^+, and g^- are both necessary and sufficient for profitability of upward/downward services.

Funded by the European Union

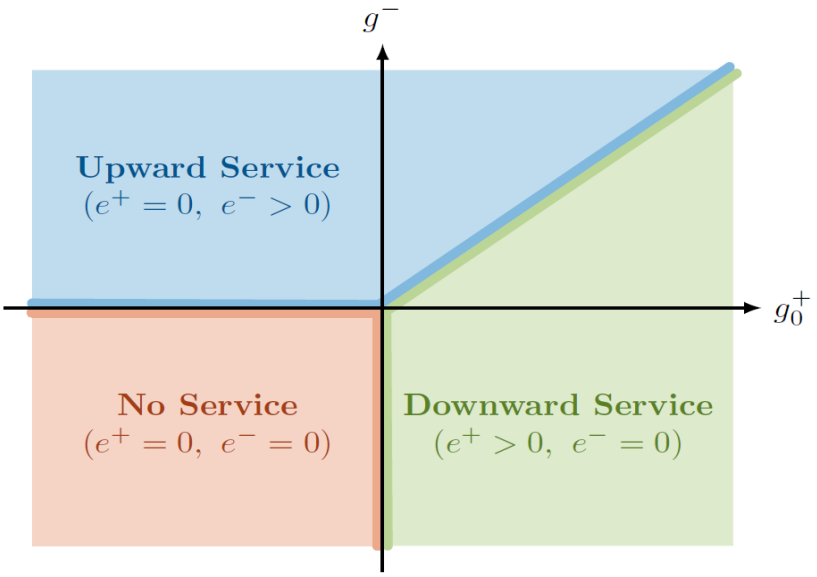

Figure 1. Partition of the (g_0^+, g^-) plane induced by the profitability conditions in the PC case. Each region represents under which conditions the service is profitable (hence offered).

To aid the interpretation, we report in Figure 1 the partition of the (g_0^+, g^-) plane induced by the edge-cases conditions. In the III quadrant $g_0^+ < 0$ and $g^- < 0$, meaning that there is no advantage in offering a downward service with respect to (w.r.t) buying energy on the DAM and there is no gain in offering an upward service instead of selling energy to the vehicle, hence the best strategy is to fully charge the vehicle buying from the DAM and not to offer any service. If $g_0^+ > 0$ and $g^- < g_0^+$, then offering a downward service instead of buying energy on the DAM is profitable, and offering an upward service is either not profitable (IV quadrant) or not as profitable as a downward one (lower part of I quadrant), hence the best strategy is to fully charge the vehicle buying Δ_e^o from DAM and $\Delta_e^{max} - \Delta_e^o$ from ASM as a downward service. Finally, if $g^- > 0$ e $g^- > g_0^+$, then offering an upward service w.r.t. selling energy to the vehicle is profitable and offering a downward service is either not profitable (II quadrant) or not as profitable as an upward one (upper part of I quadrant), hence the optimal solution is to fully charge the vehicle buying from the DAM and offer $\Delta_e^{max} - \Delta_e^o$ as an upward service.

Finally, note that the cost coefficients involved in the analysis are c^{v+}, c^{e+}, c^{s+}, and c^{s-}, while c^{e-} and c^{v-} do not appear. This is because with a single timeslot, the vehicle cannot be discharged, hence p^{dam} and p are always positive. We expect these cost coefficients to pop up in the multiple timeslot case, whose analysis is left as a future research effort.

2.3.4. Successive markets and unbalance

By solving the problem 2.11, the aggregator computes the optimal amount of energy to buy or sell on the energy and ancillary services markets. According to the setting in (Vignali, Falsone, Ruiz, & Gruosso, 2022), this decision is taken at day $t - 1$ (i.e., the day ahead) and implemented as-is in day t (i.e., the day after). However, in practice, as time goes by in day t, the aggregator can update its profile for the remaining part of day t by buying or selling energy on the so-called infra-day markets or can even choose not to follow the scheduled profile, thus unbalancing the grid. This possibility is currently not exploited in (Vignali, Falsone, Ruiz, & Gruosso, 2022), but it could be included by making $p_{k,i}$ dependent on the TSO service signal ω_s, $s = \{0, \dots, k - 1\}$, with an additive "disturbance feedback"

Funded by the European Union

term $K_{k,s,i}\ \omega_s$. The gain $K_{k,s,i}$ will still be optimized the day ahead, but it will produce a power profile $p_{k,i}$ which, at day t, changes according to the actual realization of the TSO service signal up to timeslot $k\ -\ 1$, which will be known at timeslot k of day t. This modification would increase the profitability of the ancillary services, as the following example clarifies.

Consider offering an upward ancillary service in the PC case: the analysis in Section 2.3.3 shows that it is profitable if and only if the return of selling to the ancillary services market is greater than selling to the user. When this is the case, the optimal strategy is to sell the entire (allowed by the user) vehicle capacity to the market. However, if the aggregator was allowed to unbalance, he could sell the entire capacity of the vehicles as an upward service, wait for the request by the TSO, and – afterwards – absorb the same amount of energy that has been requested by the EV users (i.e., disturbance feedback with unitary gain), eventually incurring in unbalance costs. If the unbalance cost is sufficiently small, this strategy would lead to a greater profitability, since the vehicles would depart fully charged independently on the actual realization of the TSO service signal.

2.4. Case Study

Here we make some simulations using the full-fledged framework of (Vignali, Falsone, Ruiz, & Gruosso, 2022) to show that the conditions found in Section 2.3 are sufficient also for the general case, without simplifying assumptions. Due space limits, we investigate the paid charge case only.

We consider the case of a company car park composed of $N\ =\ 100$ slots, each assigned to a single user indexed with i. The 24 hours time horizon is discretized into $T\ =\ 96$ time slots of $\tau\ =\ 15$ minutes each. Vehicle i arrives uniformly at random between 6:00 AM and 8:00 AM and leaves uniformly at random between 4:00 PM and 8:00 PM. For each vehicle i, we set $\eta_i^+\ =\eta_i^-\ =\ 0.97$, $p_i^{max}\ =-p_i^{min}\ =22\ kW$, $e_i^{min}\ =\ 0\ kWh$, and $e_i^o=0.7e_i^{max}$, with $e_i^{max}\in[40,70]$ and $e_i^o\in[0.1,0.3]kWh$ extracted at random according to a uniform distribution. The maximum power that can be exchanged with the grid is set to $p^{max}=-p^{min}=600\ kW$. The energy unitary prices[7] are shown in Figure 2 while the acceptance probabilities for the ASM are set to $\pi_k^+=0.6$ and $\pi_k^-=0.1$ for downward and upward services, respectively.

The results of our numerical investigation are summarized in Figure 3 where we report the optimal charging power profile $\sum_{i=1}^N p_{k,i}\,,k=\{1,\dots,T-1\}$, of the aggregator (bottom plots) and the corresponding working point in the $(g_0^+,\,g^-)$ plane (top plots), using day-averaged prices to compute g_0^+ and g^-, in three different cases (left to right). Different colors denote energy bought on different markets: day-ahead market (i.e., no service) (red), downward service (green), upward service (blue). Dashed line denotes the aggregate power limit. From left to right: no service case, downward service case, upward service case are reported, respectively. With the parameter values introduced before, the optimal charging policy consists in buying all the energy on the DAM and use it to fully charge the vehicles, see Figure 3 (bottom left) where the power bought by the aggregator is red (i.e., bought from DAM) at all time slots. Indeed, by considering the average energy prices and computing g_0^+ and g^-, we fall into the no-service case, as shown in Figure 3 (top left). If we now reduce the vehicle prices and set them to $c^{v+}=0.165\ €/kWh$ and $c^{v-}=0.180\ €/kWh$, then we can see that downward ancillary services become profitable, as shown in Figure 3 (top center), where the power bought by the

[7] Real Italian market data (see GME (2022)) in 2018.

Funded by the European Union

aggregator is partially in green (i.e., bought from ASM), and in Figure 3 (bottom center), where the average energy prices map into a point in the downward service area. Note that in this case also upward services are profitable ($g^- > 0$) but not as profitable as the downward ones. Finally, we raised the acceptance probability of upward services to $\pi_k^- = 0.5$ (and reduced π_k^+ to 0.5) to make upward services more profitable and we obtained the optimal aggregator power profile in Figure 3 (bottom right), where it can be seen that some time slots are blue (i.e., power bought from ASM). Accordingly, the average energy prices map into a point falling into the upward service case, see Figure 3 (top right).

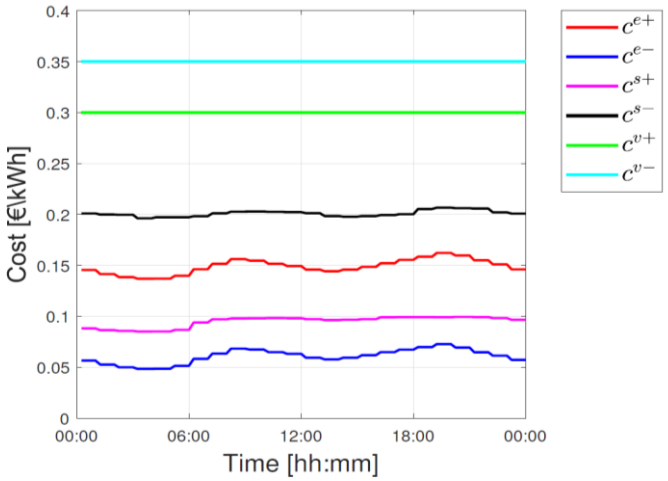

Figure 2. Day-ahead market, ancillary service market, and vehicle charging/discharging prices.

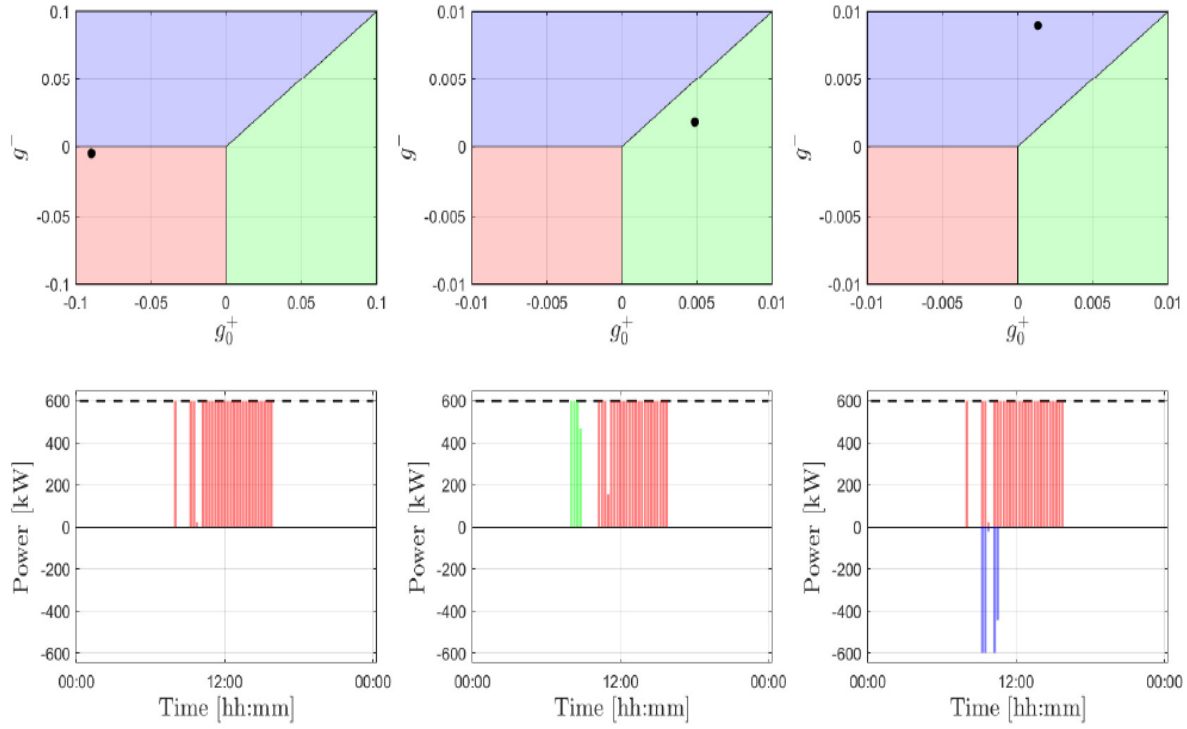

Figure 3. Top: (g_0^+, g^-) plane. Black dots are obtained by considering day-averaged prices when computing g_0^+ and g^-.

Funded by the European Union

3. Multi-objective optimization framework

This section introduces the research effort conducted in task T4.3 by adding a further level of technical detail than what is foreseen in the Executive Summary. The activity ended up with a highly customizable multi-objective optimization algorithm and base EMS for EV charging scheduling. Numerical simulations show the versatility of the algorithm and emphasize the importance of the multi-objective approach.

3.1. Modelling framework

The Julia language[8] has been chosen as the programming language for this project, as it provides high performance and offers multiple packages for mathematical optimization. Of the available modelling packages, JuMP[9] (Lubin, et al., 2023) was selected for this project. With JuMP, the problem formulation is intuitive, and it supports multiple solvers; thus, the same model (with minimal modifications) can be used with different solvers. A Mixed-Integer Linear Program (MILP) formulation is used, which is solved by Gurobi[10]. The Multi Objective Algorithms (MOAs)[11] package is used for lexicographic optimization.

3.2. Mathematical formulation

As the focus was to evaluate the multi-objective formulation, a relatively simple MILP formulation was developed for a public charging point scheduling problem based on (Mouli, Kefayati, Baldick, & Bauer, 2019).

3.2.1. Optimization variables

For each variable, j denotes the number of the EV, and t denotes the timestep. All variables are equal to or greater than zero.

$P_{EV+}^{t,j}$	Charging power of the j-th EV at timestep t [kW]
$P_{EV-}^{t,j}$	Discharging power of the j-th EV at timestep t [kW]
$E_{EV}^{t,j}$	Battery energy of the j-th EV at timestep t [kWh]
E_{unmet}^{j}	Unmet energy demand of the j-th EV (difference between the requested and actual battery energy at departure) [kWh]
P_{PV}^{t}	Used solar power at timestep t [kW]
a_{grid}^{t}	Binary variable for grid power direction (0: power fed to the grid, 1: power drawn from the grid)

[8] https://julialang.org/
[9] https://jump.dev/JuMP.jl/stable/
[10] https://www.gurobi.com/
[11] https://github.com/jump-dev/MultiObjectiveAlgorithms.jl

Funded by the European Union

P^t_{grid+}	Power fed to the grid at timestep t [kW]
P^t_{grid-}	Power drawn from the grid at timestep t [kW]
$P_{gridpeak}$	Peak power drawn during the optimization window [kW]
$P_{gridfluc}$	Peak grid power fluctuation (maximum grid power change compared to the previous timestep) [kW]

3.2.2. Constraints

Both the charging and discharging power are limited by either the converter onboard the EV or the external charger. After the EV has connected to the charger, the limits can be compared, and the stricter limit is applied.

$$P^{t,j}_{EV+} \leq P^j_{EVmax+}, \quad \forall t, \forall j, \tag{3.1}$$

$$P^{t,j}_{EV-} \leq P^j_{EVmax-}, \quad \forall t, \forall j. \tag{3.2}$$

The EV battery energy and the unmet energy demand cannot exceed the maximum battery capacity.

$$E^{t,j}_{EV} \leq E^j_{EVmax}, \quad \forall t, \forall j. \tag{3.3}$$

$$E^j_{unmet} \leq E^j_{EVmax}, \quad \forall j. \tag{3.4}$$

The used solar power is also limited by the maximum power of the panel.

$$P^t_{PV} \leq P^t_{PVmax,} \quad \forall t. \tag{3.5}$$

The battery energy at the start of the optimization is set based on the reported SoC and battery capacity of the EV. T^j_a is the arrival timestep of the j-th EV.

$$E^{T^j_a,j}_{EV} = E^j_{EVstart}, \quad \forall j. \tag{3.6}$$

At departure, the battery energy must be equal to the requested level from the EV user (E^j_{EVgoal}). The E_{unmet} term is added to avoid infeasible solutions. This is especially important with multi-objective optimization towards the extreme points on the Pareto-front. $T^j_{dep}$is the departure timestep of the j-th EV.

$$E^{T^j_{dep},j}_{EV} + E^j_{unmet} = E^j_{EVgoal}, \quad \forall j. \tag{3.7}$$

Before arrival and after departure, both the charging and discharging power are set to zero. In event-based optimization, the EVs are only added to the optimization when they arrive. In this case, it is not necessary to add constraints for the timeframe before arrival.

$$P^{t,j}_{EV+} = 0, \quad \forall t \notin [T^j_a, T^j_{dep}], \forall j. \tag{3.8}$$

Funded by the European Union

$$P_{EV-}^{t,j} = 0, \quad \forall t \notin [T_a^j, T_{dep}^j], \forall j. \tag{3.9}$$

The battery energy level for each EV for each timestep is calculated with eq. 3.10, where T_{step} is the length of one timestep in minutes, and η_{ch}^j is the converter efficiency for EV j. The charging and discharging efficiency are considered to be the same. The inclusion of this efficiency term also ensures that $P_{EV+}^{t,j}$ and $P_{EV-}^{t,j}$ are not both nonzero at the same time, the addition of a binary variable is not necessary.

$$E_{EV}^{t+1,j} = E_{EV}^{t,j} + P_{EV+}^{t,j} \frac{T_{step}}{60} \eta_{ch}^j - P_{EV-}^{t,j} \frac{T_{step}}{60 \cdot \eta_{ch}^j}, \quad \forall t \in [T_a^j, T_{dep}^j - 1]. \tag{3.10}$$

To avoid too low SoC levels, a minimum battery level is set while the EV is connected to the charger.

$$E_{EV+}^{t,j} \geq 0.2 E_{EVmax}^j, \quad \forall t \in [T_a^j, T_{dep}^j], \forall j. \tag{3.11}$$

The sum of incoming and outgoing power at each timestep must be equal to each other.

$$\sum_{j=1}^{N} P_{EV+}^{t,j} + P_{grid+}^t = P_{PV}^t + P_{grid-}^t + \sum_{j=1}^{N} P_{EV-}^{t,j} \quad \forall t, \forall j \tag{3.12}$$

P_{grid+}^t and P_{grid-}^t cannot be nonzero at the same time. While with traditional cost-only based objectives, the difference between buying and selling price can ensure this condition, with multi-objective optimization, the addition of a binary variable is necessary. $P_{gridmax}^t$ is the maximum allowed grid load at timestep t.

$$P_{grid+}^t \leq (1 - a_{grid}^t) P_{gridmax}^t, \quad \forall t, \tag{3.13}$$

$$P_{grid-}^t \leq a_{grid}^t P_{gridmax}^t, \quad \forall t. \tag{3.14}$$

3.2.3. Objectives

The objective formulations are recorded as expressions or variable-constraint combinations, and then the chosen one(s) are passed to the optimizer. This makes the algorithm highly customizable, as both the objectives and their orders can be easily modified with one parameter.

Currently, four possible objectives are defined, but more could be added. Equation 3.15 shows the cost function, where N is the number of connected EVs, T is the length of the optimization window, c_{buy}^t and c_{sell}^t denotes the electricity buying and selling price, respectively, $c_{penalty}$ is the penalty paid to the EV user for not satisfying the charging need and c_{PV} is the price for the solar power. The $c_{penalty}$ term ensures that the EVs are always charged to the requested level if it is feasible. Minimizing E_{unmet}^j could also be a separate objective.

$$min \quad \sum_{t=1}^{T} (c_{buy}^t P_{grid-}^t - c_{sell}^t P_{grid+}^t) + \sum_{j=1}^{N} c_{penalty} E_{unmet}^j + \sum_{t=1}^{T} c_{PV} P_{PV}^t. \tag{3.15}$$

Funded by the European Union

Equations 3.16 - 3.19 together describe the objective of minimizing the peak grid load. Equations 3.20 - 3.22 show the objective of minimizing the grid load fluctuations.

$$P_{grid}^{t} = P_{grid+}^{t} + P_{grid-}^{t}, \forall t, \quad 3.16$$

$$P_{grid+}^{t} \leq P_{gridpeak}, \quad \forall t, \quad 3.17$$

$$P_{grid-}^{t} \leq P_{gridpeak}, \quad \forall t, \quad 3.18$$

$$min \quad P_{gridpeak} \quad 3.19$$

$$P_{grid}^{t} - P_{grid}^{t+1} \leq P_{gridfluc} \quad \forall t \quad 3.20$$

$$P_{grid}^{t} - P_{grid}^{t+1} \geq -P_{gridfluc} \quad \forall t \quad 3.21$$

$$min \quad P_{gridfluc} \quad 3.22$$

V2G usage can increase the number of charging-discharging cycles an EV battery experiences, thus increasing the rate of battery degradation. Equations 3.23 and 3.24 try to reduce this effect by minimizing the discharged energy amount. A more detailed battery degradation model is planned to be added later.

$$E_{discharged} = \sum_{t=1}^{T} \sum_{j=1}^{N} P_{EV-}^{t,j} \frac{T_{step}}{60} \quad 3.23$$

$$min \quad E_{discharged} \quad 3.24$$

If some of these objectives are not selected, the optimizer can choose a sufficiently high value for the corresponding optimization variables, thus effectively ignoring the objective.

3.2.4. Multi-objective formulation

For the multi-objective formulation, a mathematical programming approach, the augmented ε-constraint was chosen. The implementation is based on an improved version of the method, AUGMECON2 (Mavrotas & Florios, An improved version of the augmented ε-constraint method (AUGMECON2) for finding the exact pareto set in multi-objective integer programming problems, 2013).

The augmented ε-constraint method is based on scalarization: the original multi-objective formulation is converted into a single-objective problem. With ε-constraint, one objective is optimized while the others are fixed to given values in a restricted range specified by the pay-off table. The ranges and chosen density determine the number of sub-problems that need to be solved. AUGMECON2 improves the original algorithm in two ways (Mavrotas, Effective implementation of the ε-constraint method in Multi-Objective Mathematical Programming problems, 2009).

- It guarantees the Pareto optimality of the obtained solution in the pay-off table as well as in the generation process.

Funded by the European Union

- It improves the calculation speed by introducing an early exit condition.

AUGMECON2 further enhances the speed by extracting information from the surplus variables in the formulation. It also makes it possible to produce the exact Pareto set in Multi-Objective Integer Programming (MOIP) problems (Mavrotas & Florios, An improved version of the augmented ε-constraint method (AUGMECON2) for finding the exact pareto set in multi-objective integer programming problems, 2013).

Equation 3.25 describes the general problem formulation; the notations are explained afterwards.

$$min \quad f_1(\boldsymbol{x}) + \varepsilon\left(\frac{S_2}{r_2} + 10^{-1}\frac{S_3}{r_3} + \cdots + 10^{-(n-2)}\frac{S_n}{r_n}\right) \qquad 3.25$$

$$s.t. \quad f_i(\boldsymbol{x}) - S_i = e_i \quad \forall i \in [1, N]$$

$$e_i = upper_i - \frac{iter_i\, r_i}{interval_i}$$

f_i denotes the i-th objective, N is the number of objectives. With AUGMECON2, the first step is to create the pay-off table whose size is $N \times N$. The pay-off table is filled with the objective values using the lexicographic method described in (Mavrotas, Effective implementation of the ε-constraint method in Multi-Objective Mathematical Programming problems, 2009). The minimum and maximum value for each objective determines the range of possible objective values, r_i. The maximum value determines the original upper bound, $upper_i$, which is then reduced at each iteration with a step size of $\frac{r_i}{interval_i}$, where $interval_i$ is the number of intervals in the given range (determined by the user). With more intervals (and thus grid points), a denser representation of the Pareto-front can be reached, but the computational power need also increases. The total number of sub-problems (without early exit and skipping conditions) is $\prod_{i=1}^{N}(interval_i + 1)$. Surplus variables ($S_i$) are introduced to ensure Pareto-optimality, and they can also be used to speed up the computation by skipping over grid points, which would not produce a new solution. ε is usually set between $10^{-3}$and 10^{-6} (Mavrotas, Effective implementation of the ε-constraint method in Multi-Objective Mathematical Programming problems, 2009).

In task T4.3, the above-described algorithm was implemented in a way which allows all parameters to be freely changed. This includes the number of objectives, objective order, and number of grid points for each objective. To step through all the grid points, $N-1$ nested loops are used in the original paper, where N is fixed (hard-coded). To avoid this problem, a simulated nested loop structure was implemented, where a set of slots is maintained for each looping variable using an array. This way, we avoid using recursions, which could negatively impact the performance and memory usage, but still maintain the ability to change the number of objectives only by setting a parameter (without any change in the code).

The AUGMECON2 formulation is only valid if there is a trade-off between the objectives. If there is no trade-off, the calculated range will be zero, and we run into a division by zero error. Some objectives might only conflict in certain situations (e.g., based on the electricity price, charging time, number of EVs, etc.). Thus, the algorithm was extended to automatically detect scenarios where no trade-off is present between objectives. In these cases, the objectives are removed, and their optimal values are

Funded by the European Union

added as constraints (like lexicographic optimization). If only one objective remains, the algorithm switches to single-objective optimization.

Currently, the output of the algorithm includes every found (feasible) solution and the corresponding charging schedules. To choose the most suitable solution, a higher-level Multi-Criteria Decision-Making (MCDM) algorithm will need to be developed. An iterative refinement possibility was added to help the manual selection process and for testing purposes. This means that a rough representation of the Pareto-front is first calculated, and then the decision-maker can indicate their preferred solution. Based on this information, the search space is confined, and the algorithm is run again. This iterative process continues until the decision-maker is satisfied with one of the proposed solutions.

3.2.5. Future work

In the future, the mathematical formulation will be extended to include limits for the Constant Current and Constant Voltage (CC-CV) regions during the battery charging process, as well as to allow the simulation of more general charging station setups (e.g., multiple levels of power limitations, the possibility of multiple EVs connecting to one charger).

During Task 5.3, potential ancillary services provided by EVs will be investigated. The objectives will be modified, and new objectives will be added based on the results of this investigation. This is necessary to ensure the proper co-operation between the local EMS and grid-level optimization strategy as depicted in Figure 4.

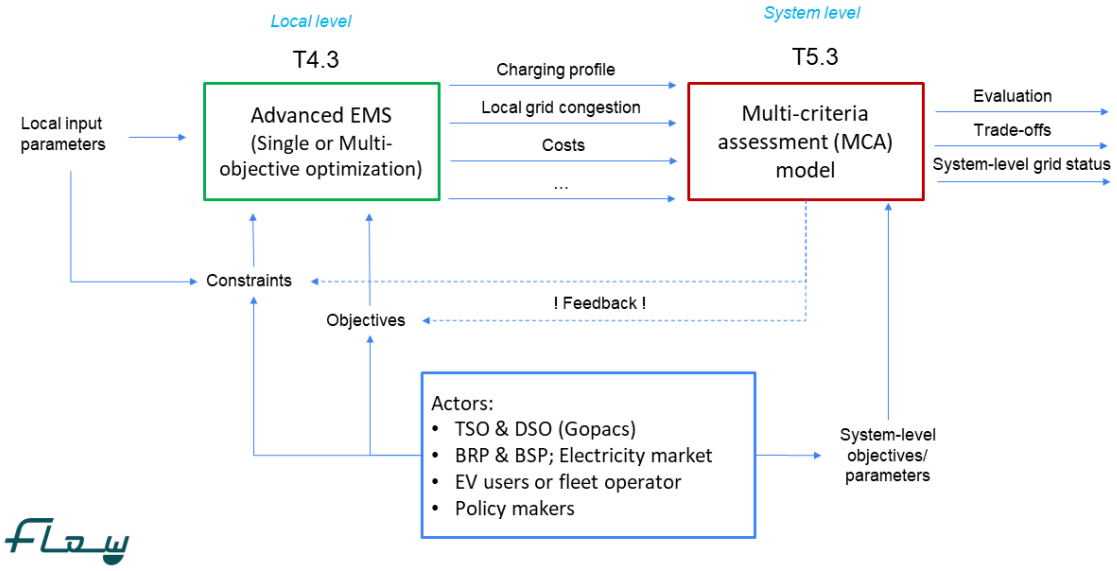

Figure 4. Connections between T4.3 and T5.3.

3.3. Energy Management System

To evaluate the previously described optimization algorithm, a simple EMS was developed. The parking lot is assumed to have solar panels and multiple chargers installed. The nominal solar power and the grid limits are configurable. The overall time window and the length of the timesteps can also be modified. Two different scheduling algorithms were developed: event-triggered and day-ahead optimization.

Funded by the European Union

3.3.1. Event-triggered scheduling

With event-triggered scheduling, we have no prior information about the EV arrival and departure times and energy demands. Departure times, current SoC and requested energy amounts are provided by the EV user after connecting to the charging station. Solar forecasts and energy prices are assumed to be available in advance.

EVs can arrive at any point during the day and are added to the arriving EVs list. At the start of the next timestep, the EVs on the list are checked against the acceptance criteria to ensure that a feasible charging schedule can be found and that constraint 3.11 is satisfied. The maximum amount of energy that can be delivered to the given EV is calculated based on the EV departure time, converter efficiency, grid limits and aggregated charging schedule of the already connected and currently connecting EVs. If the requested energy exceeds the available capacity, the EV is rejected, and the user needs to modify the scheduled departure date and/or requested energy amount. If the EV is accepted, it is added to the connected EVs list, and the optimization is re-run. The optimization window is set based on the latest departure time. After departure, the EV is removed from the connected EVs list.

Further events could be defined based on parameter changes (e.g., grid limits, forecasts, electricity prices), which trigger a re-optimization.

3.3.2. Day-ahead scheduling

Day-ahead scheduling assumes knowledge of EV-related data (arrival, departure times, SoC and energy demands) as well. This data could be provided by forecasting tools using datasets from Charging Point Operators (CPOs). The optimal schedule is calculated for a fixed time window. To combat the effects of uncertainties (forecasting errors), the optimization could be re-run periodically with updated parameters. A rolling-horizon implementation is described in (Mouli, Kefayati, Baldick, & Bauer, 2019).

3.3.3. Future work

As mentioned before, currently, no MCDM algorithm is available. Thus, either a fixed solution number is used, or the algorithm requires manual input for each iteration. The MCDM will be developed in Task 5.3. This algorithm will be capable of using inputs from the grid-level optimization strategy as well as considering the local conditions.

After the selection, the EMS updates the charging schedules for all connected EVs and resumes operation. At this time, ideal conditions are assumed, i.e., the charging process precisely follows the planned schedule. With future extensions, the grid conditions (e.g., voltage deviations) and forecast errors will also be considered.

Some EV users might not want to participate in V2G (or smart charging in general), so the algorithm must differentiate between different types of schedules (uncontrolled, unidirectional, and bidirectional smart charging).

3.4. Simulation results

To evaluate the developed framework, multiple scenarios were investigated using numerical simulations.

Funded by the European Union

3.4.1. Used datasets

The used datasets include solar data from a reference 1 kW_p panel, DAM electricity prices and EV-related data. All these datasets are reused from a previous project, Orchestrating Smart Charging in mass Deployment (OSCD) (Shekhar, Chandra Mouli, & Bauer, 2022), (Yu & al., 2022). Both the solar and price data have a 1-minute resolution for one year. The EV dataset was generated using recorded charging sessions and distribution functions from Elaad. It contains arrival and departure times, SoC (at arrival and at departure) and battery information (maximum capacity and power). The power limits (for charging and discharging) are assumed to be symmetrical.

3.4.2. Scenario 1

In scenario 1, a public charging point was considered, with 25 EVs arriving within 24 hours. Table 1 summarizes the EV-related data. The optimization timestep ($\boldsymbol{T_{step}}$) was 10 minutes. Figure 5 shows the PV forecast for the connected 20 kW_p panels. The DAM electricity prices are depicted in Figure 6. The selling price is assumed to be 90% of the buying price ($\boldsymbol{c_{sell} = 0.9 c_{buy}}$), $\boldsymbol{c_{PV}$ = 0.01 €/kWh and the penalty term $\boldsymbol{c_{penalty}}$ = 1€/kWh. The grid power limit ($\boldsymbol{P_{gridmax}}$) was set to 100kW for each timestep. The EMS was operating in day-ahead mode.

Table 1. EV data.

EV number	EV type	T_a	T_{dep}	E_{EV} at arrival	E_{EVgoal}	E_{EVmax}	P_{EVmax}
		[hh:mm]			$[kWh]$		[kW]
1	Model S	06:45	09:35	67.62	72.22	72.5	16.56
2	Model S	08:00	08:30	58.79	66.19	72.5	16.56
3	Model 3	08:45	12:25	15.82	47.12	47.5	11.04
4	Model X	08:45	14:55	62.38	72.38	72.5	16.56
5	Model 3	10:00	03:50	38.46	47.36	47.5	11.04
6	i3	10:30	02:15	30.73	37.83	37.9	11.04
7	Model S	10:45	04:25	48.6	72.5	72.5	16.56
8	Model S	10:45	17:00	55.2	72.4	72.5	16.56
9	i3	11:15	23:45	32.57	37.77	37.9	11.04
10	Model 3	11:15	05:05	43.8	47.5	47.5	11.04
11	i3	11:15	13:55	34.22	37.72	37.9	11.04
12	i3	11:30	02:35	33.67	37.77	37.9	11.04
13	Model 3	11:45	22:30	43.24	47.34	47.5	11.04
14	I-Pace	13:15	22:20	80.22	84.52	84.7	11.04
15	I-Pace	14:00	23:40	77.46	84.56	84.7	11.04
16	Model 3	14:15	18:20	38.82	47.32	47.5	11.04
17	Model 3	14:30	17:35	40.3	47.4	47.5	11.04
18	Model 3	17:30	19:25	41.4	47.4	47.5	11.04
19	Model 3	18:00	18:50	41.58	46.68	47.5	11.04
20	i3	18:15	20:30	31.65	37.85	37.9	11.04
21	Model 3	18:30	20:15	40.66	47.36	47.5	11.04
22	Model 3	18:45	00:20	37.54	47.34	47.5	11.04
23	Kona	19:00	00:05	15.64	39.14	39.2	11.04
24	i3	19:45	01:00	31.83	37.83	37.9	11.04
25	Model X	22:45	01:45	65.7	72.5	72.5	16.56

Funded by the European Union

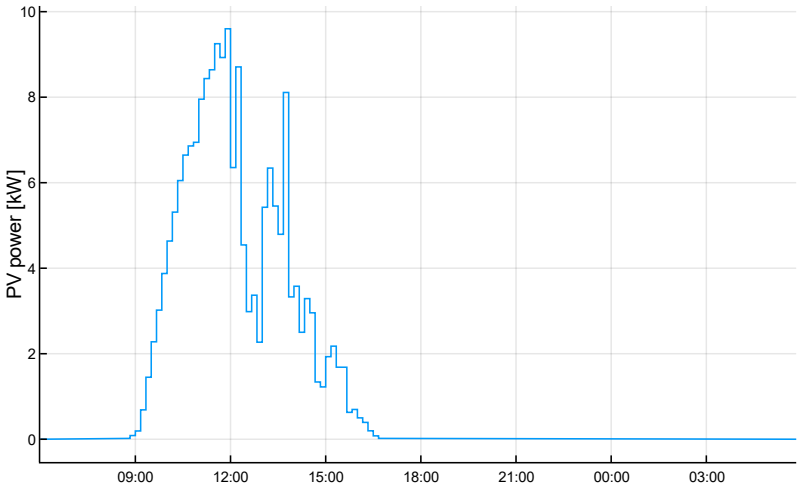

Figure 5. PV forecast.

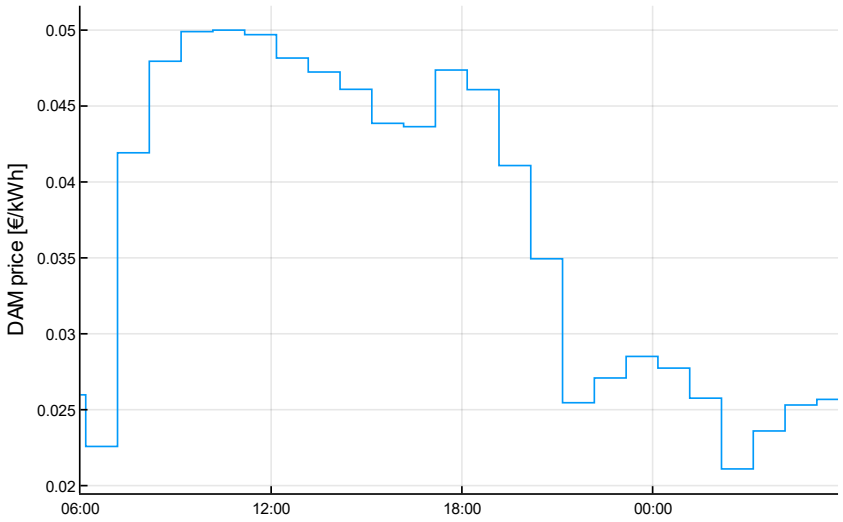

Figure 6. DAM electricity prices.

Three objectives were selected for this scenario in the following order: minimize cost, minimize peak grid load, and minimize V2G usage. The objective value ranges for objectives 2 and 3 were divided into 6 intervals, which means $7 \times 7 = 49$ maximum solutions on the Pareto-front. Figure 7 shows the calculated representation of the Pareto-front. Please note that the extreme point of $P_{gridpeak} = 0$ is not shown, as even though it is a feasible solution, it is not realistic.

Five different solutions were chosen to show the effect of the multi-objective optimization on the scheduling. Figure 8 shows the chosen points, and Table 2 gives the exact objective values. Point 1 and point 5 represent two extreme solutions for objectives 1 (lowest cost) and 3 (lowest V2G usage), respectively. There is only one extreme point for cost, as that is the main (first) objective, but there are multiple points with zero V2G usage. Solution 2 reduces the peak grid load with almost no change in V2G usage; solution 3 significantly reduces the V2G usage while keeping the peak grid load

Funded by the European Union

unaffected. Solution 4 reduces both objective values, with a minimal increase in cost compared to solution 3.

Table 2. Details of the chosen solutions for scenario 1.

Solution number	Cost [€]	Peak grid load [kW]	V2G usage [kWh]
1	30.40	100.00	234.50
2	31.15	66.67	223.46
3	38.08	100.00	78.17
4	38.32	50.00	78.17
5	45.22	60.37	0.00

The grid load profiles belonging to the different solutions are depicted in Figure 9. The effect of V2G usage reduction from solutions 3, 4 and 5 can be clearly seen at around noon. The evening grid load peak (around 21:00) is greatly reduced with solutions 2, 4 and 5.

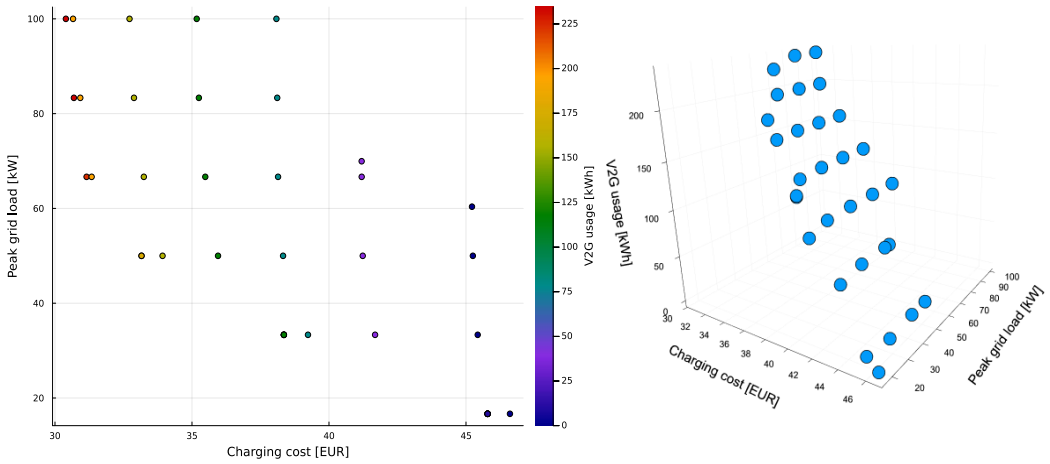

Figure 7: Pareto-front for scenario 1, left: 2D representation, right: 3D representation.

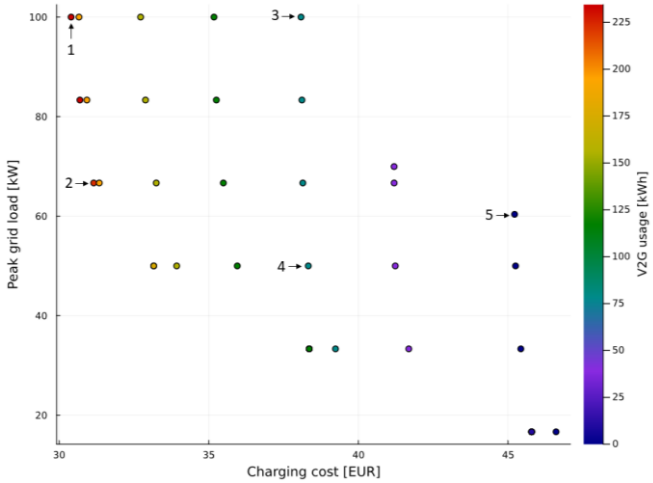

Figure 8. Chosen solutions for scenario 1.

Funded by the European Union

Figure 10 shows the power and energy profiles of one EV: with solution 1 the battery is discharged when the electricity price is high and then charged back again in the evening; solution 3 reduces the amount of discharged energy, while solution 5 completely prevents V2G usage. It is important to note that the preferred solution is highly dependent on the specific use case requirements. Therefore, there are no general suggestions that can be made.

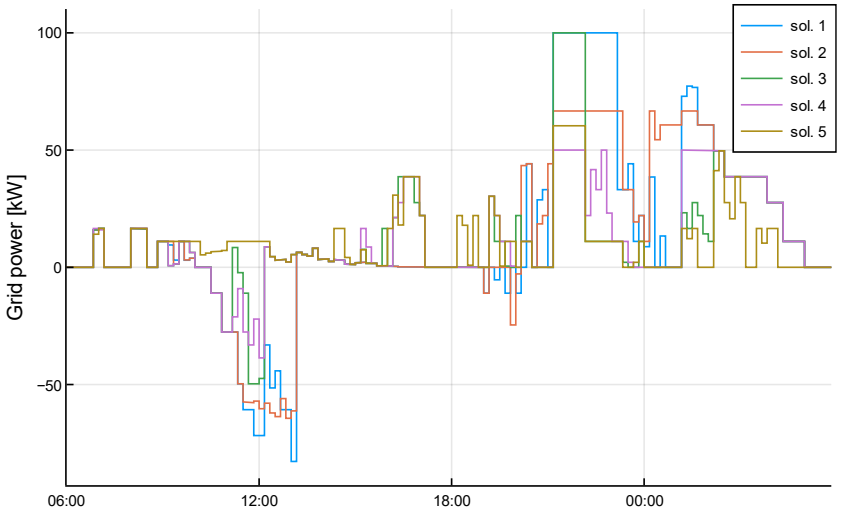

Figure 9. Grid load profiles in scenario 1.

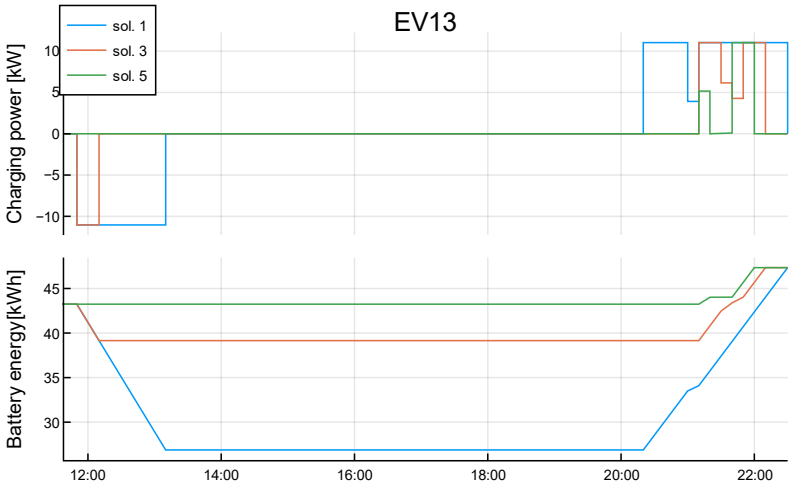

Figure 10. Battery profiles for EV13 in scenario 1.

3.4.3. Scenario 2

In scenario 2, the list of objectives was extended with the minimization of grid load fluctuations. The objective value ranges for objectives 2, 3 and 4 were divided into 4 intervals, which means $5 \times 5 \times 5 = 125$ maximum solutions on the Pareto-front. The other parameters and datasets remained unchanged. Figure 11 shows the resulting Pareto-front in the form of a ScatterPLOt Matrix (SPLOM). Part of the matrix (above the main diagonal) is omitted, as it doesn't give new information. Using this matrix, the

Funded by the European Union

relationship of any two objectives can be investigated, but the decision-making process for a human operator becomes increasingly difficult with more objectives.

Three solutions were chosen to show the effect of the fourth added objective. The details are given in Table 3. Solution 1, which focuses on cost, is the same as in scenario 1 with the addition of the load fluctuation value. Solution 2 and 3 aims to reduce the fluctuation while keeping the other objective values like solution 4 in scenario 1. A trade-off between cost and V2G usage is explored: Solution 2 provides a reduction in both the cost and the load fluctuation but increases the V2G usage. Solution 3 reduces the V2G usage (and load fluctuation) but increases the charging cost. The peak grid load remains the same in both cases. The resulting grid load profiles are shown in Figure 12.

Table 3. Chosen solutions for scenario 2.

Solution number	Cost [€]	Peak grid load [kW]	V2G usage [kWh]	Load fluctuation [kW]
1	30.40	100.00	234.50	66.88
2	36.10	50.00	117.25	16.72
3	39.79	50.00	58.62	16.72

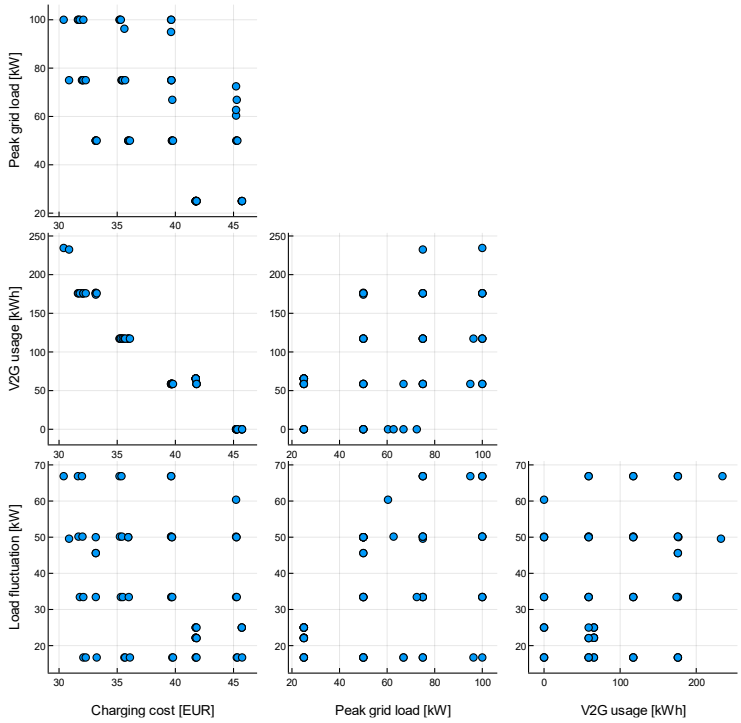

Figure 11. (Partial) SPLOM of the Pareto-front for scenario 2.

Funded by the European Union

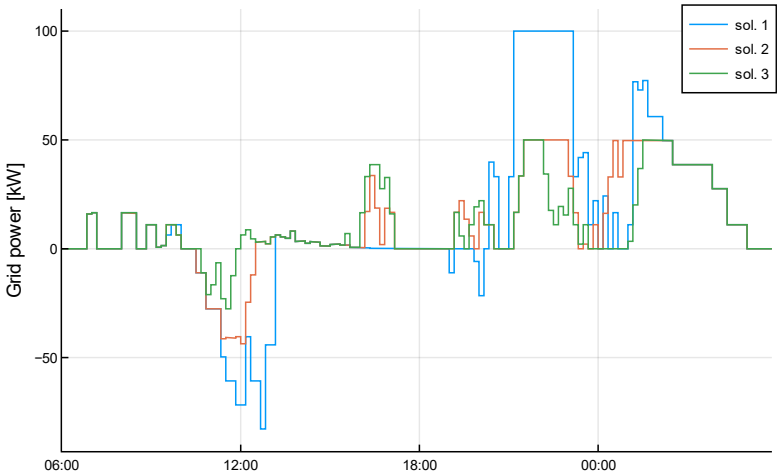

Figure 12. Grid load profiles in scenario 2.

3.4.4. Remarks

Both scenarios showcase the importance of multi-objective optimization to investigate the relationship of the objectives. A small change in one objective value might have a huge impact on the others (and thus on the overall schedule as well), but to take advantage of it, we need to first identify and quantify the potential trade-offs. The algorithm can also provide solutions to a wide array of situations without the need to add extra constraints. Modifying or adding objectives is a straightforward process, allowing great versatility.

Funded by the European Union

4. Comparing Battery Degradation Techniques in EV Charging Optimization

As highlighted in the Executive Summary, battery models are complex and their integration into EV charge optimization models is challenging. Additionally, there is a wide variety of battery technologies used in EVs, and obtaining degradation models is also difficult. All these factors, together present a substantial challenge for the Charger Station Operator (CSO). During task T4.3, various optimization models for smart charging were implemented and compared to assess the strengths and weaknesses of distinct approaches for incorporating battery degradation considerations into the optimization algorithm. The "Immediate Charging" (M0) model serves as the baseline case, representing the simplest charging approach. In this model, the EV charges at its maximum power capacity immediately after being plugged in until it reaches the predefined final SoC, without considering any price signals or degradation costs[12]. From each model, both energy costs and degradation costs are computed, and these costs are then aggregated to determine the Total Cost (TC) for each execution.

4.1. Notation

N, T, J, K	Set of charges, set of time steps, set of power piecewise degradation cost functions, and set of SoC piecewise degradation cost function
Δ_t, α, β	Time interval period, SoC threshold where maximum EV charge power decreases, and maximum power reduction factor
$Bc_{t,n}, C_t^{pch}, C_{t,n}^{bat}, C_t^u$	Battery nominal energy capacity, energy purchasing cost, battery acquisition cost, and energy purchase price
$C_{t,n,j}^P, C_{t,n,k}^{SoC}, Eff_n$	Power degradation cost per section, SoC degradation cost per section, and charger efficiency
$m, m_{SoC}, m_P,$	penalty cost to prioritize charges, penalty cost to delay chargers, and penalty cost to smooth chargers
$P_t^{I_{max}}, P_n^{ch_{max}} P_n^{ch_{min}}, P_{n,j}^{max}$	Contracted power capacity, maximum power of charger n, minimum power of charger n, and power bounds for sections of power piecewise degradation function
$SoC_{t,n}^{ini}, SoC_{t,n}^{end} SoC_n^{iniTW}, \overline{SoC} \underline{SoC}, SoC_{n,k}^{bound}$	SoC at the beginning of the charging session, SoC at the end of the charging session, SoC of the EV that is connected to charger n at the beginning of the time window optimization, maximum allowed SoC, minimum allowed SoC, and SoC bounds for each section k of SoC piecewise function
$SoH_{t,n}, U_{t,n}$	Initial SoH and forecasted charging point occupancy profile

[12] Chargers employing this method commence charging at maximum power as soon as they are connected to a charger. Immediate charging does not consider external signals like energy prices or battery degradation. This model is straightforward and commonly used, making it a suitable baseline for comparison with other models.

Funded by the European Union

$p_t^{pch}, p_{t,n}^{EV}, SoC_{t,n}$	Power purchased from the grid, charging power to the EV, and state of charge
$x_{t,n,j}^{p}, x_{t,n}^{ch}, x_{t,n,k}^{SoC}$	Binary to activate each power curve section (1 if the section is activated, 0 otherwise), binary that is activated when the battery is being charged (1 if charging, 0 no charging), and 1 if $SoC_{n,k}^{mid}$ bound is surpassed, 0 otherwise
$C_{f_{cal}}, C_{f_{cyc}}, C_{f_{total}}$	Capacity fade due to calendar ageing, capacity fade due to cycling ageing, and capacity fade due to calendar and cycling agening

4.2. Battery Degradation Model

The development of a battery degradation model plays a central role in the comparison, serving various purposes: (i) assessing degradation after each charge, (ii) integrating degradation into the optimization models, either directly or through linearization, and (iii) estimating battery life.

Table 4. Battery degradation parameters obtained in references (Olmos, et al., 2021) and (Stroe, et al., 2015).

Symbol	Value for LFP	Symbol	Value for LFP
k_{cyc}	0.003414	$mSoC_{ref}$	42%
k_T	5.8755	$Temp_{ref}$	$293K$
k_{DOD}	0.0046	a	0.869
k_{Cch}	0.1038	k_{cal}	0.1723
k_{Cdch}	0.296	k_{SoC}	0.007388
k_{mSoC}	0.0513	b	0.8

Most EV batteries are Li-ion based, and although variations exist in formats and chemistry technologies, they share common stress factors affecting their lifespan. Battery degradation modelling is intricate, with various approaches available. For brevity, additional details are provided in the cited references (Wang, et al., 2020), (Chen, Liang, Yang, & Li, 2019), (Dubarry, Qin, & Brooker, 2018), (Ecker, Käbitz, Laresgoiti, & Sauer, 2015), (Ng, Xing, & Tsui, 2014), among others. Among these modelling approaches, the semi-empirical method was chosen due to its balance between computational efficiency, data requirements, model accuracy, and ease of linearization, making it suitable for inclusion in optimization models. Numerous open-source implementations and extensive knowledge are available in the literature, such as (Redondo-Iglesias, Venet, & Pelissier, 2019), (Petit, Prada, & Sauvant-Moynot, 2016), (Smith, et al., 2017), (Omar, et al., 2014). Semi-empirical models often differentiate between Cycle aging (sensitive to operating conditions) and Calendar aging (capacity loss over time).

For the considered scenarios, a cycling model from (Olmos, et al., 2021) was selected, which includes data from various open-sources for Li-ion chemistries like Lithium Ferrum Phosphate (LFP), Nickel Manganese Cobalt (NMC), and Nickel Cobalt Aluminum (NCA), building general models for each chemistry. This model accounts for major stress factors, such as C-rate, temperature, DoD, and mean State Of Charge (mSoC). Model parameters vary based on the specific chemistry (Olmos, et al., 2021). The parameters for LFP cells are listed in Table 4. Therefore, we can write:

$$C_{f_{cyc}} = \delta_{cyc}\ FEC^{a}, \tag{4.1}$$

Funded by the European Union

where

$$\delta_{cyc} = k_{cyc}\, e^{k_T\left(\frac{T-T_{ref}}{T}\right)}\, e^{k_{DoD}\cdot DoD}\; e^{k_{C_{ch}}\cdot C_{ch}}\; e^{k_{C_{dh}}\cdot C_{dh}} \left(1 + k_{mSOC}\, mSoC \left(1 - \frac{mSoC}{2mSoC_{ref}}\right)\right). \quad 4.2$$

To address degradation during battery storage, a calendar model proposed by (Stroe, et al., 2015) for LFP cells is employed. This model considers the impact of current SoC and time on calendar aging in eq. 4.2. Hence, we can write:

$$C_{f_{cal}} = \delta_{cal}\, t^b, \quad 4.3$$

where

$$\delta_{cal} = k_{cal} \cdot e^{k_{SoC}\, SoC}. \quad 4.4$$

Combining both models, the total capacity fade experienced by the battery is calculated as:

$$C_{f_{total}} = C_{f_{cal}} + C_{f_{cyc}}. \quad 4.5$$

Both models are designed for constant stress factors. To use them with varying stress factors, the differential capacity fade for a period is computed for both cycling and calendar aging models (eqs 4.6 and 4.7). Calculating Full Equivalent Cycles (FECs) and age at the start of each period "i" is necessary. If FEC and battery age are unknown, they can be approximated using methods proposed in (Naumann, Spingler, & Jossen, 2020). These calculations allow determining the total capacity fade for each period "I" and the corresponding State of Health (SoH) (eqs 4.8--4.12).

$$dC_{f_{cyc,i}} = \delta_{cyc,i} \left(\left(FEC_{virtual_{i-1}} + FEC_i\right)^a - \left(FEC_{virtual_{i-1}}\right)^a\right), \quad 4.6$$

$$dC_{f_{cal.i}} = \delta_{cal_i} \left(\left(t_{virtual_{i-1}} + t_i\right)^b - \left(t_{virtual_{i-1}}\right)^b\right), \quad 4.7$$

$$FEC_{virtual_{i-1}} = \left(\frac{C_{f_{total,i-1}}}{\delta_{cyc_i}}\right)^{\frac{1}{a}}, \quad 4.8$$

$$t_{virtual_{i-1}} = \left(\frac{C_{f_{total,i-1}}}{\delta_{cal_i}}\right)^{\frac{1}{b}}, \quad 4.9$$

$$C_{f_{total,i-1}} = 100 - SoH_{i-1}, \quad 4.10$$

$$dC_{f_{total,i}} = dC_{f_{cal,i}} + C_{f_{cyc,i}}, \quad 4.11$$

$$SoH_i = SoH_{i-1} - dC_{f_{total,i}}. \quad 4.12$$

Additionally, the *Rainflow Algorithm* (Xu, Oudalov, Ulbig, Andersson, & Kirschen, 2018) is employed to obtain DoD and mSoC for each cycle of the profile under evaluation. The average values of other factors in each cycle are determined, considering non-zero C-rates.

To convert capacity fade ($dC_{f_{total,i}}$) into an economic indicator (Deg_{cost_i}), the battery acquisition cost (Cb) and the battery nominal energy capacity (Bc) serve as inputs. Throughout the study, it is assessed

Funded by the European Union

the reduction in battery degradation in terms of its impact on battery acquisition cost. Extending battery life reduces the need for critical materials, recycling, and landfill, leading to cost savings and reduced greenhouse gas emissions. Equation 4.13 defines the economic cost of battery degradation in each period:

$$Deg_{cost_i} = \frac{dC_{f_{total,i}}}{100 - SoH_{EOL}} Bc\ Cb. \quad 4.13$$

4.3. Model 1 (M1): Smart charging

The "Smart Charging" model considers energy prices and aims to optimize the charging process by minimizing the energy costs. By considering the fluctuating energy prices, the model strategically schedules the charging sessions to take advantage of lower electricity prices, thus reducing overall charging costs. When multiple solutions are possible, it prioritizes the charge as soon as possible.

Objective function. The objective function, shown in eq. 4.14, represents the overall cost of charging an EV. This includes the energy costs paid by the CSO associated with grid-supplied energy for all charging sessions throughout 24 hours (C_t^{pch},) and any additional fees that users pay for the energy consumed during the charging procedure (C_t^u).

$$\sum_{t \in T} \Delta_t \left(C_t^{pch}\, p_t^{pch} - \sum_{n \in N} \left(C_t^u\, p_{t,n}^{EV} + m \cdot \left(SoC_{t,n}^{end} - SoC_{n,t} \right) \right) \right). \quad 4.14$$

The expression m $\left(SoC_{t,n}^{end} - SoC_{n,t} \right)$ of the objective function represents a penalty, which aims to prioritize the charge as when multiple solutions give the same economic result. The value of m is set to be small enough so as not to influence the economic result.

Charging station constraints. Constraint 4.15 assures that every kW supplied to the charger is consumed.

$$\boldsymbol{p_t^{pch} = \sum_{n \in N} p_{t,n}^{EV}, \quad \forall t, n.} \quad 4.15$$

Constraint 4.16 limits the power supplied by the distribution network, contingent upon the contracted power capacity ($P_t{}^{I_{max}}$)

$$\boldsymbol{p_t^{pch} \leq P_t{}^{I_{max}}, \quad \forall t, n.} \quad 4.16$$

Charger constraints. The charging power can be adjusted within the domain $\left[P_n^{ch_{min}},\ P_n^{ch_{max}} \right] \cup \{0\}$. Constraints 4.17 and 4.18 define the charger power bounds.

$$\boldsymbol{p_{t,n}^{EV} \leq U_{t,n}\, P_n^{ch_{max}}\, x_{t,n}^{ch}, \quad \forall t, n,} \quad 4.17$$

$$\boldsymbol{p_{t,n}^{EV} \geq U_{t,n}\, P_n^{ch_{min}}\, x_{t,n}^{ch}, \quad \forall t, n.} \quad 4.18$$

Funded by the European Union

EV battery constraints. Constraint 4.19 guarantees the proper balance of the battery State of Charge. The actual capacity of the battery is considered using the State of Health ($SoH_{t,n}$) and the nominal battery capacity ($Bc_{t,n}$).

$$U_{t,n}\, SoC_{t,n} = \begin{cases} U_{t,n}\, SoC_n^{iniTW} + \dfrac{\Delta_t}{SoH_{t,n} \cdot Bc_{t,n}} \left(Eff_n \cdot p_{t,n}^{EV}\right), & if\ t = 1, \forall n, \\ U_{t,n}\, SoC_{t-1,n} + \dfrac{\Delta_t}{SoH_{t,n} \cdot Bc_{t,n}} \left(Eff_n \cdot p_{t,n}^{EV}\right), & \forall t > 1, n. \end{cases} \quad 4.19$$

The SoC of the battery must be maintained within an acceptable range. The upper bound is limited by constraint 4.20, and the lower bound is limited by constraint 4.21. In the final time interval during which the vehicle remains connected for charging (referred to as $t^{\star}$), the SoC must be equal to or greater than the minimum required value ($SoC_{t,n}^{end}$).

$$SoC_{t,n} \leq U_{t,n} \cdot \overline{SoC}, \quad \forall t, n, \quad 4.20$$

$$SoC_{t,n} \geq \begin{cases} U_{t,n}\, SoC, & if\ t \neq t^{\star},\ \forall n \\ SoC_{t,n}^{end}, & if\ t = t^{\star},\ \forall n \end{cases}. \quad 4.21$$

The maximum charge power depends on the battery chemistry, battery temperature, and the SoC and is controlled internally by the Battery Management System (BMS) of each vehicle (Bandara, Viera, & González, 2022). To improve the simulation of vehicle charging, a variable maximum charging power is incorporated using constraint 4.22. Figure 13 shows the impact of constraint (20), wherein the maximum charging power linearly decreases from a specified threshold.

$$p_{t,n}^{ch} \leq \begin{cases} P_{t,n}^{ch_{max}} + \dfrac{P_{t,n}^{ch_{min}} - P_{t,n}^{ch_{max}}}{1-\alpha} \left(\dfrac{SoC_{n,t}^{EV} + SoC_n^{iniTW}}{2} - \alpha\right), & if\ t = 1, \forall n \\ P_{t,n}^{ch_{max}} + \dfrac{P_{t,n}^{ch_{min}} - P_{t,n}^{ch_{max}}}{1-\alpha} \left(\dfrac{SoC_{n,t}^{EV} + SoC_{n,t-1}^{EV}}{2} - \alpha\right), & \forall t > 1, n \end{cases} \quad 4.22$$

Funded by the European Union

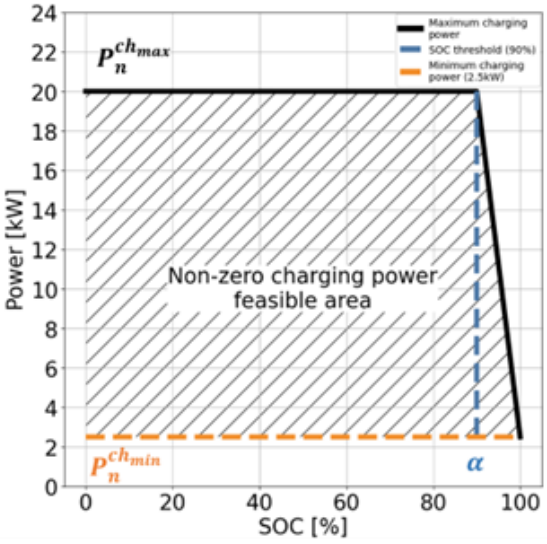

Figure 13. Feasible region for charging process.

Finally, **Model 1 (M1)** consists of the following optimization model:

$$\begin{gathered}\min\ (4.14) \\ s.t.\ (4.15), (4.16), (4.17), (4.18), (4.19), (4.20), (4.21), (4.22)\end{gathered} \qquad 4.23$$

4.4. Model 2 (M2): Good Practices for Battery Care

In situations where specific data or battery models are unavailable, it remains possible to mitigate battery degradation while keeping energy costs in check by adhering to optimal battery maintenance practices. These practices encompass tactics like delaying the charging process to prevent reaching a high SoC or reducing charging power. Model 2 represents an improvement over Model 1, as it not only considers energy pricing but also schedules charging during time periods with consistent energy costs. Our focus has been on prioritizing the following strategies.

M2.1 Smart Delayed Charging. In this variant, the cost parameter (m_{SoC}) is associated with high SoC values, prompting the model to delay full charging until the end of the period while maintaining constant costs.

$$\begin{gathered}\min \sum_{t\in T} \Delta_t \left(C_t^{pch}\, p_t^{pch} - C_t^u \sum_{n\in N} p_{t,n}^{EV} + m_{SOC} \sum_{n\in N} SoC_{n,t} \right) \\ s.t.\ (4.15), (4.16), (4.17), (4.18), (4.19), (4.20), (4.21), (4.22)\end{gathered} \qquad 4.24$$

M2.2 Smart charge with C-rate Reduction. In this variant, the cost parameter (m) is linked to the square of power, compelling the model to distribute the charging load uniformly across periods with identical costs. The squared power term penalizes charging at higher power levels, promoting even power distribution. The model problem can be represented as follows:

Funded by the European Union

$$min \sum_{t \in T} \Delta_t \left(C_t^{pch} \, p_t^{pch} - C_t^u \sum_{n \in N} p_{t,n}^{EV} + m_P \sum_{n \in N} (p_{t,n}^{EV})^2 \right) \quad 4.25$$
$$s.t. \; (4.15), (4.16), (4.17), (4.18), (4.19), (4.20), (4.21), (4.22)$$

We determined the selection of the m_P choice through a sensitivity analysis. This analysis revealed that using a value for "m" one order of magnitude lower than the smallest observed price differential achieves the objective of minimizing cost while charging at the lowest power level.

4.5. Model 3 (M3): Two-step c-rate iteration

This model signifies an enhancement over M1, specifically designed to account for the potential impact of charging on battery longevity. It achieves this through an iterative process involving M1 and the battery lifetime model. In each iteration, the power capacity is decreased, and a solution that minimizes the total cost (comprising energy cost and battery degradation cost) is pursued.

The initial step, depicted in **Figure 14**(A), involves executing the M1 model. Once M1 has computed the optimal charging power profile, the battery lifetime model is employed to assess the equivalent battery degradation cost of that solution ($C_{f_{total}}^i$).

For the subsequent iteration, as illustrated in **Figure 14**(B), the maximum charge power ($P_{t,n}^{EV_{max}}$) is reduced by β-percent (indicated by the dashed red line) in the time intervals (highlighted by the blue arrows) where the previous result exhibited the highest charge power. A potential new optimal charging profile, based on the updated maximum charge power, is presented in **Figure 14**(C). Once more, the blue arrows in **Figure 14**(C) indicate the new time intervals where the β-reduction should be applied.

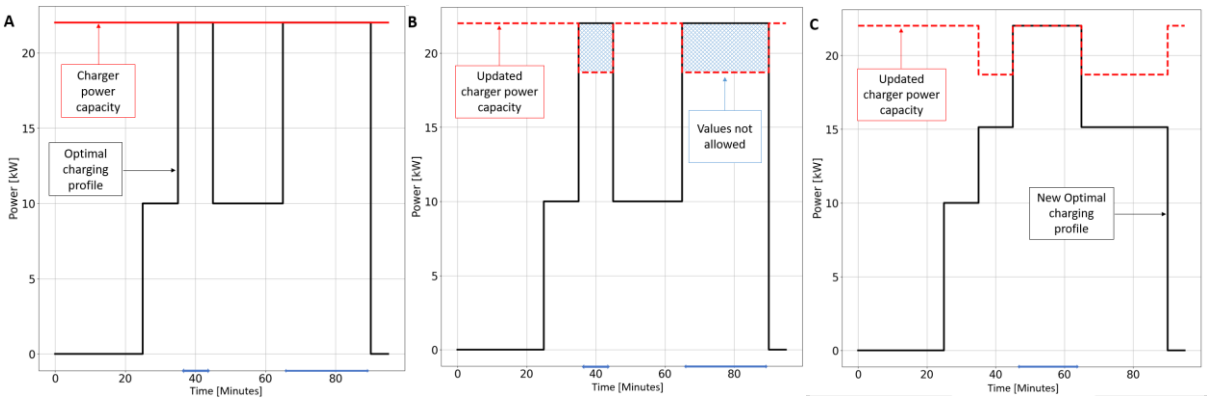

Figure 14. Example of the power constraint reduction method implemented in Model 3.

The algorithm concludes its operation when one of the following conditions is met: (i) it reaches a maximum number of iterations; (ii) it becomes impossible to attain the desired SoC with the new maximum charge power. During each iteration, the total cost ($TotalCost^i$) is computed using eq. 4.26. In this equation, $C_{f_{total}}^i$ represents the degradation cost obtained from the battery lifetime model at iteration i, C_{energy}^i signifies the cost of the energy purchased, and I_{user}^i stands for the income linked

Funded by the European Union

to user tariff prices. The result provides the total cost from the perspective of the charge station operator.

$$TotalCost^i = C^i_{f_{total}} + C^i_{energy} - I^i_{user}. \quad 4.26$$

The solution yielded by Model 3's algorithm is the optimal power profile obtained from the i-th iteration that achieves the minimum $TotalCost$.

4.6. Model 4 (M4): C-rate costs

In contrast to M3, this model eliminates the need for an iterative process between the degradation model and the smart charging problem. Instead, M3 incorporates a piece-wise linear degradation cost function into the optimization formulation. This function considers the charging power profile and allows for a more efficient optimization while considering the impact of the C-rate on battery degradation.

The rate at which a battery is charged, referred to as the C-rate, has a role in its degradation. To incorporate this concept into an optimization model, the objective function of M1 is expanded to encompass degradation costs related to a discretized C-rate parameter in J values. This enhancement enables the optimization process to consider the influence of varying C-rates on battery health.

The C-rate degradation costs are calculated using the methodology a piecewise linearization method. Based on the conditions of the charging session, the appropriate table of degradation values is selected and remains constant throughout the entire charging session.

To match the C-rate costs with the charging power variables, the C-rates are translated to power with the C-rate definition: $Power = C - rate\, Bc$. Finally, $p^{EV}_{t,n}$ will be associated with C^P_j if $p^{EV}_{t,n} \in \left(P^{max}_{t,n,j-1}, P^{max}_{t,n,j}\right]$.

Objective function. Compared with the objective function presented in eq. 4.14, a term has been included to introduce a cost according to the power delivered by charger n for each time step t, $C^P_{t,n,j} x^P_{t,n,j}$. Where $x^P_{t,n,j}$ is a binary variable used to determine in which power region $p^{EV}_{t,n}$ is contained.

$$\sum_{t \in T} \Delta_t \left(C^{pch}_t \, p^{pch}_t - \sum_{n \in N} \left(C^u_t \, p^{EV}_{t,n} - \sum_{j \in J} C^P_{t,n,j} x^P_{t,n,j} \right) \right). \quad 4.27$$

Charger constraints. The following set of constraints determines the $x^P_{t,n,j}$ variable. This variable indicates the cost region according to the charging power variable. It is assumed that for each C-rate cost table, the first row ($j = 1$) corresponds to the cost of no charging, and it is assumed to set $C^P_{t,n,1} = 0$.

$$p^{EV}_{t,n} > x^P_{t,n,j} \, U_{t,n} \, P^{max}_{nj-1}, \qquad \forall t, n, and \; \forall j > 1, \quad 4.28$$

$$p^{EV}_{t,n} \leq U_{t,n} \, P^{max}_{nj} \, x^P_{t,n,j}, \qquad \forall t, n, j, \quad 4.29$$

Funded by the European Union

$$p_{t,n}^{EV} \leq \sum_{k} x_{t,n,j}^{P} \, P_{nj}^{max}, \qquad \forall t, n, j, \tag{4.30}$$

$$\sum_{j} x_{t,n,j}^{P} \leq 1, \qquad \forall t, n, j, \tag{4.31}$$

EV Battery constraints. Finally, the Model 4 (M4): C-rate consists of the following optimization model:

$$\begin{gathered} \min \ (4.27) \\ s.t. \ (4.15), (4.16), (4.17), (4.18), (4.19), (4.20), (4.21), (4.22), \\ (4.28), (4.29), (4.30), (4.31) \end{gathered} \tag{4.32}$$

4.7. Model 5 (M5): C-rate and SOC costs

M5 aims to incorporate another factor directly affecting battery lifetime reduction: the SOC. This model builds upon Model 4 by considering the influences of both the C-rate and SoC. Like the inclusion of the C-rate cost in the model M4, M5 takes into consideration the SoC cost. The SoC degradation costs ($C_{n,k}^{SoC}$) are computed using the piecewise linearization methodology.

Objective function. In this occasion, an additional term has been added to consider the impact coming from degradation costs related to SoC: $C_{t,n,k}^{SoC} \cdot x_{t,n,k}^{SoC}$. $C_{t,n,k}^{SoC}$ represents the cost associated with having the EV plugged in at charger n at time t, where the variable $SoC_{t,n}$ belongs to the interval $(SoC_{k-1}^{mid}, SoC_{k}^{mid}]$.

$$\sum_{t \in T} \Delta_t \left(C_t^{pch} \cdot p_t^{pch} - \sum_{n \in N} \left(C_t^{u} \, p_{t,n}^{EV} - \sum_{j \in J} C_{t,n,j}^{P} x_{t,n,j}^{P} - \sum_{k \in K} C_{t,n,k}^{SoC} \cdot x_{t,n,k}^{SoC} \right) \right). \tag{4.33}$$

EV battery constraints. It is necessary to determine which values from the SoC degradation table, $C_{t,n,k}^{SoC}$, should be activated, $x_{t,n,k}^{SoC}$, according to the SoC variable, $SoC_{n,t}$. To do so, three different constraints are considered.

$$SoC_{n,t} > \ x_{t,n,k}^{SoC} \, SoC_{n,k-1}^{bound}, \qquad \forall t, n, and \ \forall k > 1, \tag{4.34}$$

$$\sum_{k} x_{t,n,k}^{SoC} \leq \ \ 1, \qquad \forall t, n, k, \tag{4.35}$$

$$SoC_{n,t} \leq \sum_{k} x_{t,n,k}^{SoC} \, SoC_{n,k}^{bound}, \qquad \forall t, n, k, \tag{4.36}$$

Finally, the Model 5 (M5): optimization problem is represented by:

$$\begin{gathered} \min \ (4.27) \\ s.t. \ (4.15), (4.16), (4.17), (4.18), (4.19), (4.20), (4.21), (4.22), \\ (4.28), (4.29), (4.30), (4.31), (4.34), (4.35), (4.36) \end{gathered} \tag{4.37}$$

Funded by the European Union

4.8. Case Study

A comprehensive case study was developed to encompass various relevant conditions that a vehicle might encounter. Since the optimal solutions of the models outlined in early sections depend on the dataset and conditions used for their execution, the case study aims to shed light on how these parameters influence the decision-making process of each model. Table 5 compiles the results of 384 scenarios executed for each individual model (Immediate Charging, M1, M2, M3, M4, and M5).

Table 5. Summary of the parameter values for the different scenarios executed.

Location (time)	Power Capacity (kW)	Initial SoC (%)	EV SoH (%)	Electricity Tariff
Office (8-15:30)	11, 22, 50, 100	25, 45, 60	85, 90, 95, 100	DP/TT
Lunch (13:30-15:30)	11, 22, 50, 100	25, 45, 60	85, 90, 95, 100	DP/TT
Shopping (16-20)	11, 22, 50, 100	25, 45, 60	85, 90, 95, 100	DP/TT
Home (20-7:30)	11, 22, 50, 100	25, 45, 60	85, 90, 95, 100	DP/TT

The parameters explored across different scenarios include:

- **Energy price signal:** The optimal solution of the models is affected by the balance between the economic benefit of shifting the charge to cheaper periods and the potential increase in degradation costs. Therefore, as illustrated in **Figure 15**, this study compares the following two energy price structures during a weekday:
    - **Time of Use Tariff (TT):** A commercial tariff (6.1 TDVE) with different prices (P3, P4, P6) within a weekday in June 2023. ("Tarifa Períodes," 2023)
    - **Dynamic Prices (DP):** A tariff with an hourly price signal: Spanish regulated energy price as of April 28th, 2023 ("ESIOS electricidad," 2023).
- **Location and parking time:** Charger usage times have been adapted based on four locations: Office, Lunch, Shopping, and Home. The time scheduling of each location is represented by the colored boxes in **Figure 15**.
- **Initial and final SoC:** To ensure a consistent and standardized comparison across all scenarios and models, a uniform energy requirement of 20kWh for all charging sessions was established. Consequently, the final SoC values for each scenario based on this energy requirement were calculated along with the three different initial SoC values, defined as 25%, 45%, and 60%.
- **EV battery SoH:** Given the exponential nature of the selected battery model, battery degradation is more pronounced when the battery has a higher SoH. Therefore, the case study includes different SoH levels to facilitate comparison.
- **Maximum charger power (Maximum C-rate):** Four common values for charger capacities (11, 22, 50, 100kW) were considered, resulting in C-rate values of 0.22C, 0.44C, 1C, and 2C, respectively. While it is currently uncommon for home chargers to have 50 or 100kW capacities, these scenarios were included in the test matrix for completeness.

Funded by the European Union

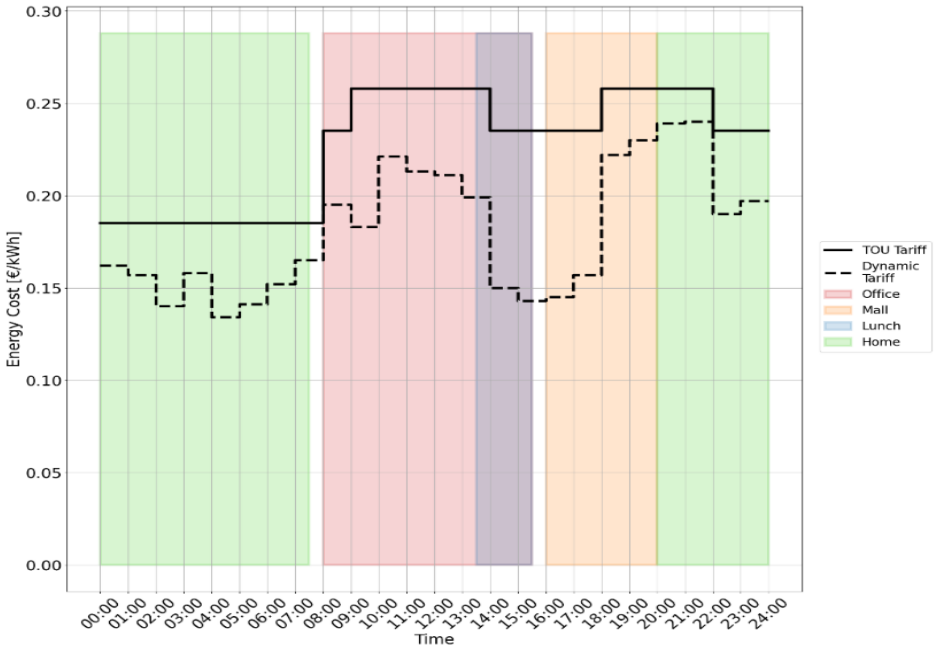

Figure 15. Energy prices signals combined with the Location and Parking Time.

The results were acquired using a computer with an Intel© Core™ i7-7800X CPU and 32GB of RAM. Furthermore, the various optimization models were implemented and solved using the Pyomo Python[13] package and the open-source solver SCIP[14].

The simulations show that scenarios characterized by longer parking durations, higher SoH, higher charger powers, and stable price signals (TT tariffs) show a greater potential for improving TC Reduction compared to Model 1 (M1). These findings underscore the importance of prioritizing the implementation of optimization models that account for battery degradation when managing a Charging Station. However, it is worth noting that in some scenarios, certain proposed models may increase energy costs while reducing battery degradation costs. This highlights the delicate balance between the interests of the CSO in lowering their costs and the interests of vehicle owners in minimizing their total costs, which include both energy costs and battery degradation costs.

Table 6 summarizes various indicators for each model, revealing that the implementation of smart charging, with or without considering degradation costs, has the potential to significantly reduce total costs compared to “Immediate Charging”, with reductions ranging from 13.4% to 14.6%. Additionally, the incorporation of degradation models for managing unidirectional charging (V1G) can further reduce costs, with reductions ranging from 0.88% to 1.39% compared to M1.

Concerning execution time, most models exhibited efficient execution times, except for M3 and M5. M3, due to its iterative nature, demonstrated low variability in execution time, with a standard deviation of 19.68 seconds. In contrast, M5 exhibited longer and more variable execution times, with an average execution time higher than M3 and a standard deviation of 394.95 seconds. This suggests that the execution time of M5 is significantly influenced by the specific scenario, while M3's execution

[13] https://www.pyomo.org/
[14] https://www.scipopt.org/

Funded by the European Union

time remains relatively consistent across scenarios. The extended duration for M5 is primarily attributed to specific "Home" scenarios. In two instances, namely (charger power: 50kW, SoH: 95%, initial SoC: 60%) and (charger power: 100kW, SoH: 90%, initial SoC: 25%), the solver reached the one-hour execution time limit without achieving an optimal solution, resulting in an optimality gap of 0.09% and 0.15%, respectively.

Table 6. Comparison of the different models with the indicators obtained throughout the results. Colors reflect the locations (i.e., "Office", "Mail", "Lunch, and "Home") as depicted in Figure 15. Red, orange and green colors are also intentionally used to refer to the quality of the obtained results.

	Im. Charg. (M0)	Smart Charg. (M1)	Delayed Sm. Mod. (M2.1)	C-rate reduc. (M2.2)	Two-steps (M3)	C-rate (M4)	C-rate & SoC (M5)
Avg. Total Cost	5.67 €	4.87 €	4.79 €	4.81 €	4.78 €	4.81 €	4.78 €
Avg. Cost reduction vs. Im. Charg.	-	13.38%	14.47%	14.27%	14.61%	14.16%	14.54%
Avg. Cost reduction vs. M1	-	-	1.22%	1.00%	1.39%	0.88%	1.31%
Avg. execution Time (sec)	-	0.146s	0.205s	0.737s	43.3s	0.972s	91.3s
Degradation Data required	No data required	No data required	General battery care	General battery care	Full model	One table	Two tables

Each of the methods explored in this study requires distinct sets of data. Some of this data pertains to user preferences, such as preferred departure time or desired SoC, which are essential for enabling smart charging. To incorporate degradation considerations, a model of the vehicle battery system is necessary, either in its full form (as in M3) or in its linearized form (M4 and M5).

4.9. Summary of battery degradation assessment

In this study, it has been examined the potential of integrating battery degradation considerations into EV smart charging algorithms, discovering that it offers cost reduction and battery lifespan extension benefits even in unidirectional charging scenarios. It has been established baseline models ("Immediate Charging" and M1) and developed variations, some implicitly considering degradation (M2) and others explicitly incorporating it (M3, M4, and M5). Analyzing these models revealed substantial Total Cost Reduction (TCR) potential, especially when compared to "Immediate Charging" ("Immediate Charging"). Transitioning from M0 to optimal models resulted in a TCR of 13.4% to 14.6%, while the proposed models achieved a TCR of 0.88% to 1.39% compared to M1.

CSOs often overlook degradation impacts, focusing on cost reduction and customer experience. In contrast, customers seek to lower ownership costs and extend battery life. This distinction could lead to a "Smart and Healthy" battery charging business model for operators. Sensitivity analysis highlighted the importance of the SoC stress factor, with SoC-based models (M2, M3, and M5)

Funded by the European Union

outperforming C-rate-based ones (M2 and M4). However, SoC-based models require more data and time. Higher degradation rates and stable electricity tariffs, such as Time of Use (ToU), enhance cost reduction potential. Higher charger power capacities lead to greater reductions.

The work carried within task T4.3 identifies method benefits and challenges, with M3 often performing well but not guaranteed to be the lowest cost option due to its heuristic nature. M5 can over- or underestimate degradation cost due to linearization. Yet, both models extract additional value compared to basic smart charging. Future work includes exploring motivations of vehicle owners and station operators, conducting simulations in larger charging stations, and extending models to bidirectional charging scenarios.

Funded by
the European Union

5. Conclusions

In conclusion, deliverable D4.3 provided a comprehensive overview of the research efforts and findings from months M4 to M18 within task T4.3 of the FLOW project. The primary focus of this task was to design advanced smart charging solutions to facilitate the integration of EVs into electric power systems.

As highlighted in the analysis presented, deliverable D4.3 underscores the critical significance of Vehicle-To-Everything technology and sheds light on the complexities inherent in Energy Management Systems. These foundational concepts serve as springboard for delving into advanced EMS capabilities.

This prompted further research into quantifying the economic benefits of Vehicle-to-Grid energy management frameworks. Through a rigorous analysis based on previous work by project partners, we successfully quantified the economic advantages associated with providing ancillary services to the grid. Our analysis has also established necessary and sufficient conditions for profitability, illustrated through numerical simulations using MATLAB.

Additionally, deliverable D4.3 encompasses the development of a highly flexible multi-objective optimization algorithm and a foundational EMS for scheduling EV charging. Leveraging Mixed-Integer Linear Program formulations, these innovations offer adaptability and scalability for broad deployment. Numerical simulations using JuMP and Gurobi as the solver have convincingly demonstrated the effectiveness of the multi-objective approach.

Finally, deliverable D4.3 investigated the intricate challenges associated with integrating battery models into EV charge optimization systems. These complexities stem from the wide array of battery technologies utilized in EVs and task of acquiring degradation models. The performed investigation centered on the evaluation of various optimization models tailored for smart charging, with a specific emphasis on the inclusion of battery degradation considerations. The ultimate findings underscore the essential need for comprehensive optimization models to improve charging practices by considering the significance of the SoC stress factor.

The findings and advancements unveiled in deliverable D4.3 lay a robust foundation for ongoing efforts to enhance EMS capabilities, accommodate uncertainties, explore battery degradation models, and address multi-criteria optimization challenges. As EVs continue to assume a more significant role in the energy landscape, these contributions are poised to drive the realization of a sustainable and dependable electric mobility ecosystem, closely aligning with the objectives of the FLOW project.

Funded by the European Union

References

Ahmadi, B., Arias, N. B., Hoogsteen, G., & Hurink, J. L. (2022). Multi-objective Advanced Grey Wolf optimization Framework for Smart Charging Scheduling of EVs in Distribution Grids,". *57th International Universities Power Engineering Conference: Big Data and Smart Grids, UPEC 2022 - Proceedings*, (pp. 1-6).

Ahmadian, A., Sedghi, M., Mohammadi-ivatloo, B., Elkamel, A., Aliakbar Golkar, M., & Fowler, M. (2018). Cost-Benefit Analysis of V2G Implementation in Distribution Networks Considering PEVs Battery Degradation. *IEEE Transactions on Sustainable Energy*, 961-970.

Alipour, M., Mohammad-Ivatloo, B., Moradi-Dalvand, M., & Zare, K. (2017). Stochastic scheduling of aggregators of plug-in electric vehicles for participation in energy and ancillary service markets. *Energy*, 1168-1179.

Association, I. E. (2023, 9 5). *Global EV Outlook 2023*. Retrieved from https://www.iea.org/reports/global-ev-outlook-2023

Bai, Y., Wang, J., & He, W. (2022). Energy arbitrage optimization of lithium-ion battery considering short-term revenue and long-term battery life loss. *Energy Reports*, 364-371.

Bandara, T., Viera, J., & González, M. (2022). The next generation of fast charging methods for Lithium-ion batteries: The natural current-absorption methods. *Renewable and Sustainable Energy Reviews*, 112338.

Baure, G., & Dubarry, M. (2020). Durability and Reliability of EV Batteries under Electric Utility Grid Operations: Impact of Frequency Regulation Usage on Cell Degradation. *Energies*, 1-11.

Bessa, R. J., & Matos, M. A. (2012). Economic and technical management of an aggregation agent for electric vehicles: a literature survey. *European transactions on electrical power*, 334-350.

Bianchi, F., Falsone, A., & Vignali, R. (2023). Vehicle-to-Grid and ancillary services: a profitability analysis under uncertainty. *22nd IFAC World Congress* (pp. 7659-7665). Yokohama, Japan: Elsevier.

Calvillo, C., Czechowski, K., Soder, L., Sanchez-Miralles, A., & Villar, J. (2016). Vehicle-to-grid profitability considering EV battery degradation. *2016 IEEE PES Asia-Pacific Power and Energy Engineering Conference (APPEEC)* (pp. 310-314). Xi'an, China: IEEE.

Chan, C. (2007). The state of the art of electric, hybrid, and fuel cell vehicles. *Proceedings of the IEEE*, 704-718.

Chen, W., Liang, J., Yang, Z., & Li, G. (2019). A Review of Lithium-Ion Battery for Electric Vehicle Applications and Beyond. *Energy Procedia, Innovative Solutions for Energy Transitions*, 4363-4368.

Chiandussi, G., Codegone, M., Ferrero, S., & Varesio, F. E. (2012). Comparison of multi-objective optimization methodologies for engineering applications. *Computers & Mathematics with Applications*, 912-942.

Funded by the European Union

Chung, C.-H., Jangra, S., Lai, Q., & Lin, X. (2020). Optimization of Electric Vehicle Charging for Battery Maintenance and Degradation Management. *Transactions on Transportation Electrification*, 958-969.

Chung, H., Li, W., Yuen, C., Wen, C., & Crespi, N. (2019). Electric Vehicle Charge Scheduling Mechanism to Maximize Cost Efficiency and User Convenience. *IEEE Transactions on Smart Grids*, 3020-3030.

Coello Coello, C. A., Lamont, G. B., & Van Veldhuizen, D. A. (2007). *Evolutionary Algorithms for Solving Multi-Objective Problems.* Springer.

Cohon, J., & Marks, D. (1975). A review and evaluation of multiobjective programming techniques. *Water Resources Research*, 208-220.

Das, R., Wang, Y., Putrus, G., Kotter, R., Marzband, M., Herteleer, B., & Warmerdam, J. (2020). Multi-objective techno-economic-environmental optimisation of electric vehicle for energy services. *Applied Energy*, 113965.

De Los Rıos, A., Goentzel, J., Nordstrom, K., & Siegert, C. (2012). Economic analysis of vehicle-to-grid (v2g)-enabled fleets participating in the regulation service market. *2012 IEEE PES nnovative Smart Grid Technologies (ISGT)* (pp. 1-8). Washington, DC, USA: IEEE.

DeForest, N., MacDonald, J. S., & Black, D. (2018). Day ahead optimization of an electric vehicle fleet providing ancillary services in the Los Angeles Air Force Base vehicle-to-grid demonstration. *Applied Energy*, 987-1001.

Dubarry, M., Qin, N., & Brooker, P. (2018). Calendar aging of commercial Li-ions cells of different chemistries - A review. *Current Opinion in Electrochemistry*, 106-113.

Ecker, M., Käbitz, S., Laresgoiti, I., & Sauer, D. (2015). Parameterization of a Physico-Chemical Model of a Lithium-Ion Battery: II. Model Validation. *Journal of The Electrochemical Society*, A1849-A1857.

Einaddin, A. H., & Yazdankhah, A. S. (2020). novel approach for multi-objective optimal scheduling of large-scale EV fleets in a smart distribution grid considering realistic and stochastic modeling framework. *International Journal of Electrical Power & Energy Systems*, 105617.

Farzin, H., Fotuhi-Firuzabad, M., & Moeini-Aghtaie, M. (2016). A Practical Scheme to Involve Degradation Cost of Lithium-Ion Batteries in Vehicle-to-Grid Applications. *IEEE Transactions on Sustainable Energy*, 1730-1738.

García-Miguel, P., Alonso-Martínez, J., Arnaltes Gómez, S., García Plaza, M., & Asensio, A. (2022). A Review on the Degradation Implementation for the Operation of Battery Energy Storage Systems . *Batteries*, 1-11.

Garcia-Villalobos, J., Zamora, I., Knezovic, K., & Marinelli, M. (2016). Multi-objective optimization control of plug-in electric vehicles in low voltage distribution networks. *Applied Energy*, 155-168.

Funded by the European Union

Garcia-Villalobos, J., Zamora, I., SAn Martin, J., Asensio, F., & Aperribay, V. (2014). Plug-in electric vehicles in electric distribution networks: A review of smart charging approaches. *Renewable and Sustainable Energy Reviews*, 717-731.

Heilmann, C., & Friedl, G. (2021). Factors influencing the economic success of grid-to-vehicle and vehicle-to-grid applications - a review and meta-analysis. *Renewable and Sustainable Energy Reviews*, 111115.

Hoke, A., Brissette, A., Smith, K., Pratt, A., & Maksimovic, D. (2014). Accounting for lithium-ion battery degradation in electric vehicle charging optimization. *IEEE Journal of Emerging and Selected Topics in Power Electronics*, 691-700.

Jafari, M., Gauchia, A., Zhao, S., Zhang, K., & Gauchia, L. (2018). Electric Vehicle Vattery Cycle Aging Evaluation in Real-Word Daily Driving and Vehicle-To-Grid Services. *IEEE Transactions on Transportation Electrification*, 122-134.

Jiang, R., Zhang, Z., Li, J., Zhang, Y., & Huang, Q. (2017). A coordinated charging strategy for electric vehicles based on multi-objective optimization. *2nd International Conference on Power and Renewable Energy*, (pp. 823-827).

Kapoor, A., Gangwar, P., Sharma, A., & Mohapatra, A. (2020). Multi-objective framework for optimal scheduling of electric vehicles. *21st National Power System Conference*, (pp. 1-6).

Kaur, K., Singh, M., & Kumar, N. (2019). Multiobjective optimization for frequency support using electric vehicles: An aggregator-based hierarchical control mechanism. *IEEE Systems Journal* , 771-782.

Kharra, A., Tiwari, R., Singh, J., & Rawat, T. (2023). Interval Optimization Technique Based Multi-Objective Scheduling of Electric Vehicles. *2023 International Conference on Power, Instrumentation, Energy and Control (PIECON)*, (pp. 1-6).

Leippi, A., Fleschutz, M., & Murphy, M. (2022). A Review of EV Battery Utilization in Demand Response Considering Battery Degradation in Non-Residential Vehicle-to-Grid Scenarios. *Energies*, 3227.

Liu, C., Chau, K., Wu, D., & Gao, S. (2013). Opportunities and challenges of vehicle-to-home, vehicle-to-vehicle, and vehicle-to-grid technologies. *Proceedings of the IEEE*, 2409-2427.

Liu, C., Chau, K., Wu, D., & Gao, S. (2018). Opportunities and Challenges of Vehicle-to-Home, Vehicle-to-Vehicle, and Vehicle-to-Grid Technologies. *Proceedings of the IEEE*, 2409-2427.

Liu, S., & Etemadi, A. H. (2018). A Dynamic Stochastic Optimization for Recharging Plug-In Electric Vehicles. *IEEE Transactions on Smart Grid*, 4154-4161.

Lubin, M., Dowson, O., Garcia, J. D., Huchette, J., Legat, B., & Vielma, J. P. (2023). JuMP 1.0: recent improvements to a modeling language for mathematical optimization. *Mathematical Programming Computation* , 581–589.

Maheshwari, A., Paterakis, N., Santarelli, M., & Gibescu, M. (2020). Optimizing the operation of energy storage using a non-linear lithium-ion battery degradation model. *Applied Energy*, 114360.

Funded by the European Union

Maigha, & Crow, M. (2018). Electric vehicle scheduling considering co-optimized customer and system objectives. *IEEE Transactions on Sustainable Energy*, 410-419.

Mal, S., Chattopadhyay, A., & Yang, A. G. (2013). Electric vehicle smart charging and vehicle-to-grid operation. *International Journal of Parallel, Emergent and Distributed Systems*, 249-265.

Martins, R., Hesse, H., Jungbauer, J., Vorbuchner, T., & Musilek, P. (2018). Optimal Component Sizing for Peak Shaving Battery Energy Storage System for Industrial Applications. *Energies*, 1-11.

Mavrotas, G. (2009). Effective implementation of the ε-constraint method in Multi-Objective Mathematical Programming problems. *Applied Mathematics and Computation*, 455-465.

Mavrotas, G., & Florios, K. (2013). An improved version of the augmented ε-constraint method (AUGMECON2) for finding the exact pareto set in multi-objective integer programming problems. *Applied Mathematics and Computation*, 9652-9669.

Mishra, S., Mondal, A., & Mondal, S. (2022). A Multi-Objective Optimization Framework for Electric Vehicle Charge Scheduling With Adaptable Charging Ports. *IEEE Transactions on Vehicle Technology*, 5702-5714.

Mouli, G., Kefayati, M., Baldick, R., & Bauer, P. (2019). Integrated PV charging of EV fleet based on energy prices, V2G, and offer of reserves. *IEEE Transactions on Smart Grids*, 1313-1325.

Naumann, M., Spingler, F., & Jossen, A. (2020). Analysis and modeling of cycle aging of a commercial LiFePO4/graphite cell. *Journal of Power Sources*, 227666.

Ng, S., Xing, Y., & Tsui, K. (2014). A naive Bayes model for robust remaining useful life prediction of lithium-ion battery. *Applied Energy*, 114-123.

Nimalsiri, N., Mediwaththe, C., Ratnam, E., Shaw, M. S., & Halgamuge, S. (2019). A survey of algorithms for distributed charging control of electric vehicles in smart grid. *IEEE Transactions on Intelligent Transportation Systems*, 4497-4515.

Olmos, J., Gandiaga, I., Saez-de-Ibarra, A., Larrea, X., Nieva, T., & Aizpuru, I. (2021). Modelling the cycling degradation of Li-ion batteries: Chemistry influenced stress factors. *Journal of Energy Storage* , 102765.

Omar, N., Monem, M., Firouz, Y., Salminen, J., Smekens, J., Hegazy, O., . . . Van Mierlo, J. (2014). Lithium iron phosphate based battery Assessment of the aging parameters and development of cycle life model. *Applied Energy*, 1575-1585.

Pecas Lopes, J., Joel Soares, F., & Rocha Almeida, P. (2010). Integration of Electric Vehicles in the Electric Power System. *Proceedings of the IEEE*, 168-183.

Petit, M., Prada, E., & Sauvant-Moynot, V. (2016). Development of an empirical aging model for Li-ion batteries and application to assess the impact of Vehicle-to-Grid strategies on battery lifetime. *Applied Energy*, 398-407.

Porras, A., Fernández-Blanco, R., Morales, J., & Pineda, S. (2020). An Efficient Robust Approach to the Day-Ahead Operation of an Aggregator of Electric Vehicles. *IEEE Transactions on Smart Grid*, 4960-4970.

Funded by the European Union

Prencipe, L., van Essen, J., Caggiani, L., Ottomanelli, M., & Homem de Almeida Correia, G. (2022). A mathematical programming model for optimal fleet management of electric car-sharing systems with Vehicle-to-Grid operations. *Journal of Cleaner Production*, 1-18.

Recalde Melo, D., Trippe, A., Gooi, H., & Massier, T. (2018). Robust Electric Vehicle Aggregation for Ancillary Service Provision Considering Battery Aging. *IEEE Transactions on Smart Grid*, 1728-1738.

Redondo-Iglesias, E., Venet, P., & Pelissier, S. (2019). Efficiency Degradation Model of Lithium-Ion Batteries for Electric Vehicles. *IEEE Transactions on Industrial Applications*, 1932-1940.

Rosewater, D., Copp, D., Nguyen, T., Byrne, R., & Santoso, S. (2019). Battery Energy Storage Models for Optimal Control. *IEEE Access*, 178357-178391.

Ruzika, S., & Wiecek, M. (2005). Approximation methods in multiobjective programming. *Journal of Approximation Methods in Multiobjective Programming*, 473-501.

Saez-de-Ibarra, A., Martinez-Laserna, E., Stroe, D.-I., Swierczynski, M., & Rodriguez, P. (2016). Sizing Study of Second Life Li-ion Batteries for Enhancing Renewable Energy Grid Integration. *IEEE Transactions on Industrial Applications*, 4999-5008.

Shekhar, Y., Chandra Mouli, G., & Bauer, P. (2022). Comparative Impact of Three Practical Electric Vehicle Charging Scheduling Schemes on Low Voltage Distribution Grids. *Energies*, 8722.

Shi, R., Li, S., Zhang, P., & Lee, K. (2020). Integration of renewable energy sources and electric vehicles in V2G network with adjustable robust optimization. *Renewable Energy*, 1067-1080.

Singh, J., & Tiwari, R. (2018). Multi-Objective Optimal Scheduling of Electric Vehicles in Distribution System. *20th National Power Systems Conference (NPSC)*, (pp. 1-6).

Singh, J., & Tiwari, R. (2020). Cost Benefit Analysis for V2G Implementation of Electric Vehicles in Distribution System. *IEEE Transaction on Industrial Applications*, 5963-5973.

Singh, P., Das, S., Wen, F. P., Singh, A., & Thakur, P. (2023). Multi-objective planning of electric vehicles charging in distribution system considering priority-based vehicle-to-grid scheduling. *Swarm Evolution Computation*, 101234.

Smith, K., Saxon, A., Keyser, M., Lundstrom, B., Cao, Z., & Roc, A. (2017). Life prediction model for grid-connected Li-ion battery energy storage system. *American Control Conference* (pp. 4062-4068). Seattle, WA, UAS: IEEE.

Sortomme, E., & El-Sharkawi, M. (2011). Optimal scheduling of vehicle-to-grid energy and ancillary services. *IEEE Transactions on Smart Grid*, 351-359.

Sovacool, B., & Hirsh, R. (2009). Beyond batteries: an examination of the benefits and barriers to plug-in hybrid electric vehicles (PHEVs) and a vehicle-to-grid (V2G) transition. *Energy Policy*, 1095-10103.

Sovacool, B., Axsen, J., & Kempton, W. (2017). Tempering the Promise of Electric Mobility? A Sociotechnical Review and Research Agenda for Vehicle-Grid Integration (VGI) and Vehicle-to-Grid (V2G). *Annual Review of Environment and Resources*, 16-30.

Funded by the European Union

Sriyakul, T., & Jermsittiparsert, K. (2020). Optimal economic management of an electric vehicles aggregator by using a stochastic p-robust optimization technique. *Journal of Energy Storage*, 1-9.

Stroe, D.-I., Swierczynski, M., Stroe, A.-I., Teodorescu, R., Laerke, R., & Kjaer, P. (2015). Degradation behaviour of Lithium-ion batteries based on field measured frequency regulation mission profile. *EEE Energy Conversion Congress and Exposition* (pp. 14-21). Montreal, QC, Canada: IEEE.

Sun, W., Neumann, F., & Harrison, G. P. (2020). Robust Scheduling of Electric Vehicle Charging in LV Distribution Networks Under Uncertainty. *IEEE Transactions on Industry Applications*, 5785-5795.

Tan, K. M., & Ramachandaramurthy, V. Y. (2016). Integration of electric vehicles in smart grid: A review on vehicle to grid technologies and optimization techinques. *Renewable and Sustainable Energy Reviews*, 720-732.

Thomposon, A. (2018). Economic implications of lithium ion battery degradation for Vehicle-to-Grid (V2X) services. *Journal of Power Sources*, 691-709.

Vignali, R., Falsone, A., Ruiz, F., & Gruosso, G. (2022). Towards a comprehensive framework for V2G optimal operation in presence of uncertainty. *Sustainable Energy, Grids and Networks*, 1-15.

Wang, Y., Jiao, X., & Sun, Z. L. (2017). Energy Management Strategy in Consideration of Battery Health for PHEV via Stochastic control and Particle Swarm Optimization Algorithm. *Energies*, 1894.

Wang, Y., Tian, J., Sun, Z., Wang, L., Xu, R., Li, M., & Chen, Z. (2020). A comprehensive review of battery modeling and state estimation approaches for advanced battery management systems. *Renewable and Sustainable Energy Reviews*, 110015.

Wei, Z., Li, Y., & Cai, L. (2018). Electric Vehicle Charging Scheme for a Park-and-Charge System Considering Battery Degradation Costs. *IEEE Transactions on Intelligent Vehicles*, 361-373.

Williams, J., De Benedictis, A., Ghanadan, R., Mahone, A., Moore, J., & Morrow, W. (2012). The technology path to deep greenhouse gas emissions cuts by 2050: the pivotal role of electricity. *Science*, 53-59.

Xu, B., Oudalov, A., Ulbig, A., Andersson, G., & Kirschen, D. (2018). Modeling of Lithium-Ion Battery Degradation for Cell Life Assessment. *IEEE Transactions on Smart Grid*, 1131-1140.

Yu, Y., & al., e. (2022). Data-Driven Study of Low Voltage Distribution Grid Behaviour with Increasing Electric Vehicle Penetration. *IEEE Access*, 6053-6070.

Zakariazadeh, A., Jadid, S., & Siano, P. (2014). Multi-objective scheduling of electric vehicles in smart distribution system,. *Energy Conversion and Management*, 43-53.

Zhao, C., & Li, X. (2023). Microgrid Optimal Energy Scheduling Considering Neural Network based Battery Degradation. *IEEE Transaction on Power Systems*, 1-12.

Funded by the European Union